nature communications

Article

https://doi.org/10.1038/s41467-025-56418-4

# Simultaneous aerobic and anaerobic respiration in hot spring chemolithotrophic bacteria

Received: 3 May 2024

Accepted: 16 January 2025

Published online: 27 January 2025

Check for updates

Lisa M. Keller, Daniel R. Colman & Eric S. Boyd

Aerobic and anaerobic organisms and their functions are spatially or temporally decoupled at scales ranging from individual cells to ecosystems and from minutes to hours. This is due to competition for energy substrates and/or biochemical incompatibility with oxygen ($O_2$). Here we report a chemolithotrophic Aquificales bacterium, *Hydrogenobacter*, isolated from a circumneutral hot spring in Yellowstone National Park (YNP) capable of simultaneous aerobic and anaerobic respiration when provided with hydrogen ($H_2$), elemental sulfur ($S^0$), and $O_2$. Cultivation experiments demonstrated that simultaneous aerobic and anaerobic respiration enhanced growth rates and final cell concentrations when compared to those grown aerobically or anaerobically. Consumption of $O_2$ measured via gas chromatography and detection of transcripts for proteins involved in $S^0$ and $O_2$ reduction in $H_2/S^0/O_2$-grown cultures confirmed co-occurring aerobic and anaerobic metabolism. This aerobic, $S^0$-reducing metabolism is suggested to provide a competitive advantage in environments where $O_2$ availability is low and variable. Genomic data indicating the prevalence of proteins allowing for this hybrid form of energy metabolism among bacteria and archaea suggest it to be widespread but previously overlooked due to rapid, $O_2$-dependent abiotic oxidation of produced sulfide. These observations challenge existing paradigms of strict delineations between aerobic and anaerobic metabolism.

The order Aquificales is an early diverging bacterial lineage that is most commonly found in high temperature hydrothermal systems where it is often predominant in microbial communities[1–5]. This includes dark, deep-sea hydrothermal vents and continental hot springs that have conditions that often preclude photosynthetic metabolisms[6,7]. As such, Aquificales tend to be microaerophiles that can oxidize hydrogen ($H_2$), arsenite, sulfide ($H_2S/HS^-$), or $H_2S/HS^-$ oxidation products such as thiosulfate ($S_2O_3^{2-}$) and elemental sulfur ($S^0$) to drive chemolithoautotrophic metabolism[8]. Exceptions include facultatively anaerobic members that can also reduce nitrate, arsenate, and ferric iron or those that can also grow chemoorganotrophically[9–16].

The predominance of microaerophilic and obligately or facultatively chemolithoautotrophic Aquificales in many hot spring environments is consistent with the availability of oxidants (e.g., $O_2$), reductants (e.g., $H_2$, $HS^-$, $S^0$), and $CO_2$ in these habitats and the generally limited availability of organic carbon[17,18]. This includes acidic hot springs that are typically sourced by oxidized meteoric water (recent rain or snowmelt) that can be infused by volcanic gas rich in $CO_2$ and reductant such as $H_2S$ and $H_2$[19–21]. In such environments, the Aquificales genus *Hydrogenobaculum*, which grows autotrophically via aerobic oxidation of $H_2$, $H_2S/HS^-$, or $S^0$, often predominates[1,22–25]. Likewise, circumneutral to alkaline hot springs, which tend to be sourced by deep hydrothermal aquifers, often host communities comprised of the Aquificales genera *Thermocrinis* and *Sulfurihydrogenibium* that grow autotrophically via aerobic oxidation of $H_2$, $HS^-$, $S^0$, or $S_2O_3^{2-}$[1,10,11,14,26–28]. These bacteria can form abundant filamentous biofilms in the outflow

Department of Microbiology and Cell Biology, Montana State University, Bozeman, MT, USA. e-mail: eric.boyd@montana.edu

channels of hot springs[2,29,30], positioning themselves near the air water interface to maximize access to atmospheric $O_2$. This is an important emergent function since deep aquifer waters that source circumneutral to alkaline hot springs tend to be anoxic[19] due to their long residence times in the subsurface[31,32]. However, many circumneutral to alkaline hot springs lack outflow channels and availability of $O_2$ is limited to atmospheric gas infusion that is enhanced by turbulence created through volcanic gas ebullition and geysing. Yet, the planktonic (water column) communities in these pools, and to a lesser extent the sediment communities, still tend to be dominated by members of the Aquificales, including those related to the aerobic members of *Thermocrinis*, *Venenivibrio*, and *Hydrogenobacter*[33–38]. This suggests the possibility of alternative adaptations or growth strategies that allow these organisms to successfully compete for energy resources, even when $O_2$ is limited.

*Thermocrinis ruber* strain OC 1/4 was isolated from Octopus Spring, an alkaline spring in the Lower Geyser Basin of Yellowstone National Park (YNP), U.S.A.[28]. *T. ruber* is a microaerophilic autotroph that can oxidize $H_2$, $S_2O_3^{2-}$, and $S^0$. Interestingly, in the presence of $H_2$, *T. ruber* was reported to reduce $S^0$ to $HS^-$ when $O_2$ concentrations were low (< 3% vol./vol). However, it was not reported if this was due to $O_2$ being preferentially consumed prior to commencement of $S^0$ reduction. Similarly, *Aquifex aeolicus*, which was isolated under $H_2$-oxidizing microaerophilic conditions[39], has been reported to reduce $S^0$ to $HS^-$ with $H_2$ as a reductant during growth in the presence of $O_2$[40]. Cells were also reported to not grow in anaerobic conditions. Biochemical data from a previous study indicates that energetic coupling of the oxidation of $H_2$ with the reduction of $S^0$ in *A. aeolicus* occurs via a membrane-bound [NiFe]-hydrogenase (Hyd)-sulfur reductase (Sre) complex (Hyd-Sre), with electron transfer from $H_2$ via quinone to a molybdopterin cofactor in Sre[40]. *T. ruber* also encodes Hyd and Sre (genome assembly ASM51273v1), suggesting that $S^0$ reduction with $H_2$ is likely occurring via this complex, and that this is apparently not inhibited by $O_2$. The growth and $HS^-$ production in *A. aeolicus* and *T. ruber* via the $H_2/S^0$ couple in the presence of $O_2$[28,40] suggests low levels of $O_2$ could enhance growth and activity in these organisms. Generating a better understanding of this putative hybrid aerobic/anaerobic respiratory strategy would provide insight into how phylogenetically deep-branching facultatively aerobic microorganisms successfully compete in environments where $O_2$ flux is low and variable both today and in similar environments on early Earth as it became oxygenated.

To begin to investigate this phenomenon, an Aquificales strain, herein referred to as *Hydrogenobacter* RSW1, that inhabits a hot spring sourced by deep, anoxic hydrothermal waters and that is capable of microaerophilic growth and $H_2$-dependent $S^0$ reduction was isolated and characterized with respect to aerobic and anaerobic growth. Analyses of the RSW1 isolate genome were used to predict the metabolic potential of *Hydrogenobacter* RSW1, which included an ability to oxidize $H_2$ and $S^0$ and an ability to reduce $S^0$ and $O_2$ based on proteins encoded. Here we describe this strain and characterize its growth kinetics when provided with various combinations of these electron donor and acceptor pairs, including when provided with multiple electron donors or acceptors at the same time. Results are discussed as they relate to the ecology of this widespread group of organisms and the putative insights these data provide into how anaerobic cells may have adapted to take advantage of $O_2$ as it became progressively more available.

## Results and discussion

### Roadside west (RSW) description

In June of 2017, RSW had a temperature of ~68 °C and a pH of ~6.8. The temperature and pH have been relatively stable since 1996, ranging from 62 to 70 °C and in pH from 6.44 to 6.80[17,41–44]. The $HS^-$ and Fe(II) concentrations were 0.44 mg $L^{-1}$ (13.3 μM) and below the limit of detection (LOD; 0.011 mg/L), respectively, at the time of sampling. The concentration of $SO_4^{2-}$ was 72 mg $L^{-1}$ ( ~ 750 μM) and the concentration of $Cl^-$ was 370 mg $L^{-1}$ ( ~ 10 mM). These values suggest that RSW is sourced by the deep hydrothermal aquifer (estimated to contain 30–70 mg $L^{-1}$ $SO_4^{2-}$ and 300 mg $L^{-1}$ $Cl^-$[19,20,43]) with minimal input of near surface meteoric water, as shown in previous studies[43]. Consistent with this interpretation, the $\delta^2H$ and $\delta^{18}O$ values of RSW waters have ranged from −130 to −132‰ and −12.0 to −12.5‰[17,41,43,44], similar to other hot springs sourced by the deep hydrothermal aquifer and that have undergone boiling and evaporation[19,20,43]. As such, the hydrothermal fluids sourcing RSW are likely to be anoxic[19] due to their long ( ~ 100's to 1000's years) residence time in the subsurface[32].

The spring is fairly turbulent due to volcanic gas ebullition (including $CO_2$ and $H_2$[44]) that likely promotes infusion of atmospheric gas (i.e., $O_2$). Previous reports of hydrogen peroxide ($H_2O_2$) in the source of RSW range from 119 to 156 nM. $H_2O_2$ is produced via photochemical reactions involving dissolved organic carbon (DOC) and $O_2$, implying available $O_2$. Further, the $H_2O_2$ and DOC values in RSW are similar to another spring in YNP where dissolved $O_2$ (DO) was measured at concentrations ranging from 152 to 165 μM. Although DO measurements were not taken during the original sampling event in 2017, DO measurements were collected in October of 2024 using a DO instrument and $O_2$ probe. The probe was tested prior to field measurements to ensure accuracy by measuring $O_2$ concentration while increasing the temperature in a water bath (Supplementary Fig. 3A). Once the probe functionality was confirmed, measurements were collected in the water column of RSW (68 °C, pH 6.57 at time of sampling) every 30 sec over a span of 10 min. DO values ranged from 77.5 to 96.9 μM in the water column of the spring (Supplementary Fig. 3B) and were around 12.5 μM at a depth of 0.5 cm into the sediment. This suggests that $O_2$ may become limiting to microorganisms in the water column and sediments of the spring. Based on metagenomic sequencing of the planktonic and sediment communities, a diverse set of organisms capable of aerobic, anaerobic, and $S^0$ metabolisms were identified[43]. Together, these observations make RSW an appropriate target for understanding the interplay between anaerobic and aerobic thermophile metabolisms.

### *Hydrogenobacter* RSW1 description and phylogenetic position within aquificales

Three rounds of dilution to extinction enrichments using $S^0$-rich sediments from RSW[44] as inoculum and medium containing $H_2$ as an electron donor, $O_2$ as an electron acceptor, and $CO_2$ as a carbon source yielded a culture with a single morphotype. A genome was assembled from sequenced culture DNA that comprised 48 contigs and that was estimated to be 98.0% complete; 5% of reads were unbinned. 99.9% of the raw reads were classified as *Hydrogenobacter* using SingleM[45], confirming that the culture is an isolate. The genome (*Hydrogenobacter* RSW1) was most closely related to the Aquificales bacterium *Hydrogenobacter hydrogenophilus*[24], formerly known as *Calderobacterium hydrogenophilum*[46]. The genome of *Hydrogenobacter* RSW1 exhibited an average nucleotide identity (ANI) of 86.8% and an average amino acid identity (AAI) of 88.7% to the *H. hydrogenophilus* genome and encoded proteins, respectively, suggesting that it represented an undescribed species within the *Hydrogenobacter* genus.

A phylogenomic analysis was conducted with members of the Aquificales (NCBI accession numbers can be found in Supplementary Fig. 2), rooted with members of the Thermotogales (Fig. 1; Supplementary Fig. 2), as has been done in previous analyses of the Aquificales[47]. *Hydrogenobacter* RSW1 groups with other YNP *Hydrogenobacter* metagenome assembled genomes (MAGs), all of which are descended from an ancestor of *H. hydrogenophilus* and *H. thermophilus*. The close shared ancestry between the *Thermocrinis* and *Hydrogenobacter* clades indicates that these organisms are likely metabolically similar and therefore may share similar metabolic, physiological, and ecological traits.

https://doi.org/10.1038/s41467-025-56418-4

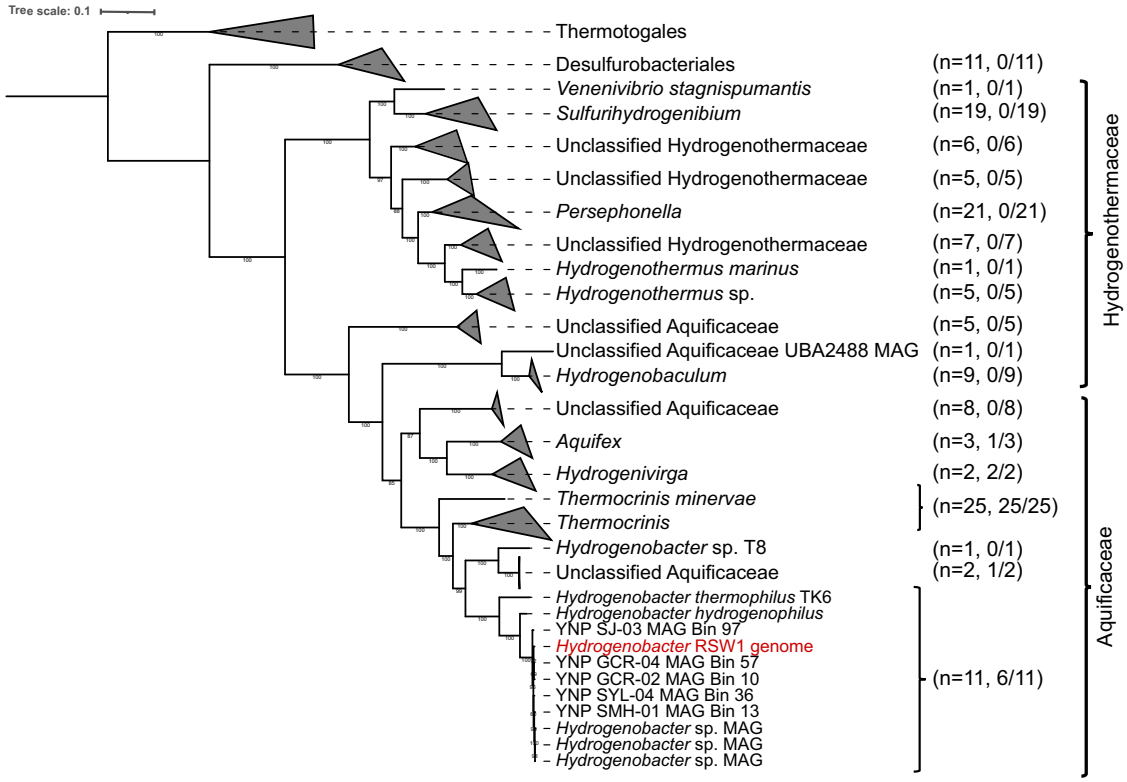


**Fig. 1 | Phylogenomic reconstruction of members of the orders Aquificales and Desulfurobacteriales, with the distribution of sulfur reductase subunit A (SreA) homologs indicated.** Desulfurobacteriales are grouped at the order level, while *Hydrogenobacter* is grouped at the species level; all other Aquificales clades are grouped at the genus level, except where MAGs could not be classified to a known genus. The total number of organisms within each clade (n) is indicated, followed by the number of organisms within those clades that encode homologs of SreA. *Hydrogenobacter* RSW1 is depicted in bold, red text. Members of the order Thermotogales were used as the outgroup. The uncollapsed phylogeny, along with accession numbers, are provided in Supplementary Fig. 2.

The order Desulfurobacteriales branches distinctly and basal from other Aquificales, which are further classified as the families Hydrogenothermaceae and Aquificaceae. Members of the Desulfurobacteriales can reduce $S^0$[9,48–52] but apparently do so through mechanisms that do not involve Sre since homologs of this enzyme are not encoded in their genomes (Fig. 1). Interestingly, Desulfurobacteriales also contain the only members that have been characterized as obligate anaerobes[9,48], while all members within Aquificales, which includes the families Aquificaceae and Hydrogenothermaceae, are considered to be microaerophiles, with some being facultative anaerobes[8,10,11,13,14,22,26–28,39,40,53,54]. As such, the ability to utilize $O_2$ as an oxidant appears to have occurred after the divergence of Aquificales from Desulforobacteriales, with all derived lineages apparently capable of using $O_2$. Homologs of proteins involved in $S^0$ respiration (Sre) were acquired in Aquificales post divergence of Hydrogenothermaceae and Aquificaceae from their ancestor, as indicated by the distribution of homologs in the latter family and their paucity in the former (Fig. 1). Among members of Aquificaceae, the distribution of Sre is widespread with 100% of the *Thermocrinis* genomes, 50% of the *Hydrogenobacter* genomes, and all *Hydrogenivirga* genomes analyzed encoding homologs of Sre, while three clades of Unclassified Aquificaceae do not encode for Sre.

To further interrogate the ecology of *Hydrogenobacter* RSW1, protein encoding genes in its genome were annotated to predict its metabolic potential. The RSW1 genome encodes a full reductive TCA (rTCA) cycle for $CO_2$ fixation, consistent with isolation of the strain with $CO_2$ as the sole provided carbon source and with many members in the order Aquificales being autotrophic[2,55,56]. The genome of *Hydrogenobacter* RSW1 does not encode identifiable organic carbon importers and lacks full glycolytic and TCA cycles, but does encode a full gluconeogenesis pathway (Fig. 2), indicating that this organism is potentially an obligate autotroph, consistent with the strain identified as most closely related[46]. Efforts to grow this organism using a variety of organic carbon sources (formate, acetate, glucose, fructose, galactose, mannose, lactose, maltose, sucrose, yeast extract, peptone, casamino acids) under microaerophilic conditions in the presence or absence of $H_2$ as an electron donor were unsuccessful. The *Hydrogenobacter* RSW1 genome encodes a variety of sulfur metabolizing genes, including a homolog of Sqr (sulfide quinone oxidoreductase). The RSW1 genome also encodes the sulfur oxidation (Sox) system, including SoxAX, SoxYZ, and SoxB, indicating the ability to oxidize both $S^0$ and $S_2O_3^{2-}$ to $SO_4^{2-}$[57]. In addition to $S^0$ oxidation pathways, the RSW1 genome encodes SreABC (sulfur reductase), an enzyme complex allowing for the reduction of $S^0$ or polysulfide ($S_x^{2-}$) to $HS^-$[40,58,59], with SreA being the catalytic subunit. The absence of a twin arginine motif in the N-terminus of SreA suggests that it is localized on the cytoplasmic side of the cell membrane, requiring $S^0$ or $S_x^{2-}$ to be transported across the cell membrane (Fig. 2). The RSW1 genome does not encode dissimilatory $SO_4^{2-}$ reduction genes, indicating that cells cannot generate energy from $SO_4^{2-}$ reduction.

The *Hydrogenobacter* RSW1 genome also encodes three homologs of [NiFe]-hydrogenases including representatives of group 1e, 1 d, and 2 d hydrogenase[60] (Fig. 2). The group 1e hydrogenase (Hydrogenase 1) is predicted to supply reducing equivalents to the $S^0/S_x^{2-}$ reducing Sre complex, which was first isolated and described in the Aquificales bacterium *Aquifex aeolicus*[40], and that is distributed among numerous other bacterial and archaeal organisms[58,59,61–63]. The group 1 d hydrogenase (Hydrogenase 2) is predicted to be involved in $H_2$ oxidation coupled to reduction of $O_2$ and is thus likely involved in aerobic respiration. Lastly, the group 2 d hydrogenase (Hydrogenase 3) is hypothesized to be involved in generating reducing equivalents (i.e., NAD(P)H) for $CO_2$ fixation, although the exact function has not been

https://doi.org/10.1038/s41467-025-56418-4

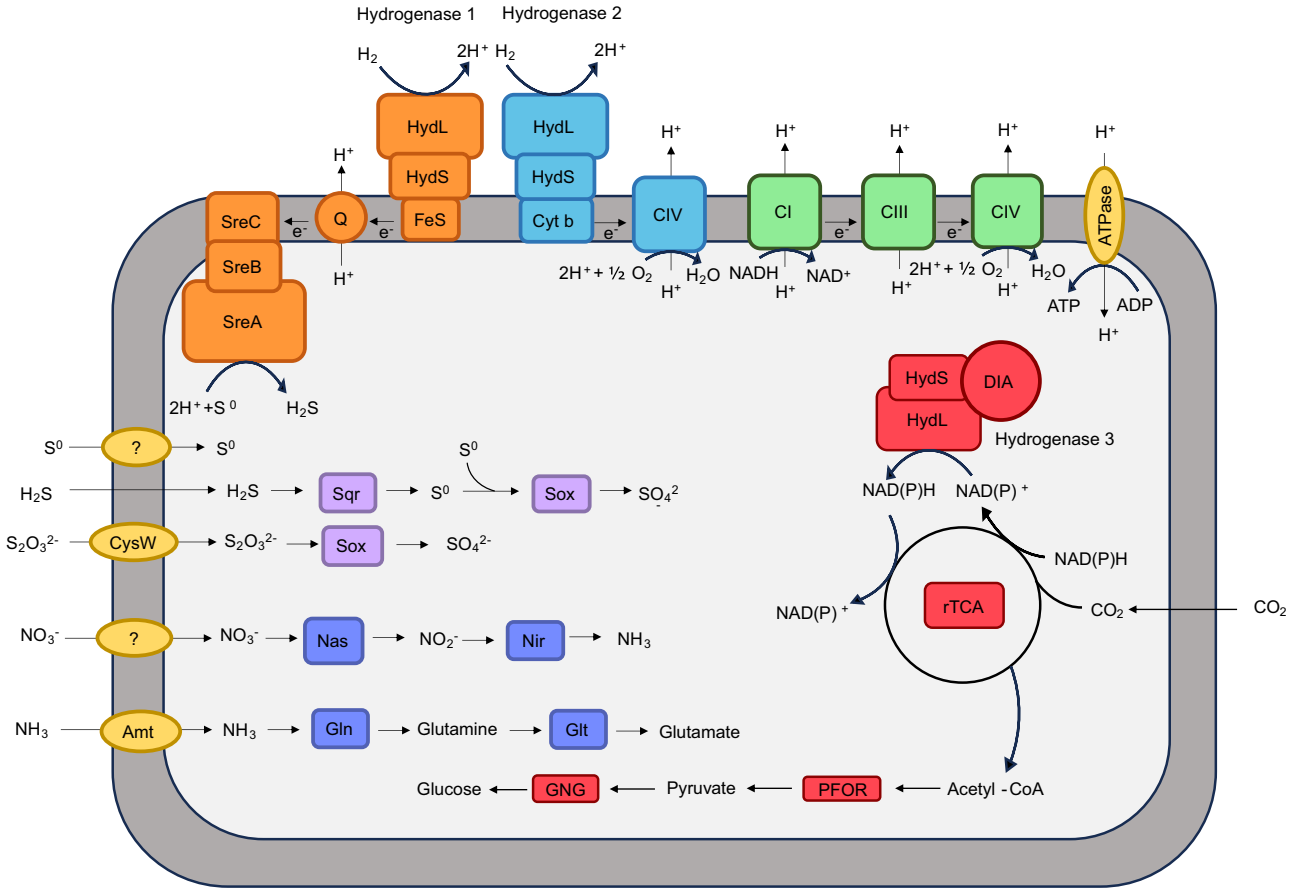


**Fig. 2 | Simplified model of relevant metabolic capabilities of *Hydrogenobacter* strain RSW1 based on genome annotation, physiological assays, and literature describing closely related strains.** Amt, ammonia transporter; CI, complex 1; CIII, complex 3; CIV, complex 4 (Cox); CysW, sulfate/thiosulfate ABC transporter; Cyt B, cytochrome B subunit; DIA, diaphorase subunit; Gln, glutamine synthetase; Glt, glutamate synthase; GNG, gluconeogenesis; HydS, hydrogenase small subunit; HydL, hydrogenase large subunit; Nas, assimilatory nitrate reductase; Nir, nitrite reductase; PFOR, pyruvate: ferredoxin oxidoreductase; Q, quinone pool; rTCA, reductive TCA cycle; Sqr, sulfide quinone oxidoreductase; Sox, sulfur oxidation (Sox) pathway; Sre, sulfur reductase. Proteins related to sulfur oxidation (purple), sulfur reduction (orange), nitrogen assimilation (dark blue), carbon fixation (red), hydrogen oxidation (light blue), and oxidative phosphorylation (green) are color coded respectively. Transport proteins are yellow. Pathways are depicted to only show metabolisms discussed in the text. Question marks indicate uncertainty in how those depicted tasks are performed.

identified[60]. Consistent with this prediction, a diaphorase subunit that facilitates electron transfer to/from NAD(P)H is encoded by a gene proximal to the group 2 d hydrogenase enzyme (Fig. 2).

### *Hydrogenobacter* RSW1 growth characterization

Genomic predictions of the metabolism of RSW1 were tested experimentally, in particular the ability to oxidize $HS^-$, $S^0$, and $S_2O_3^{2-}$ under microaerobic (2% vol./vol. $O_2$) conditions. Equations are provided to refer to throughout the results and discussion:

$$2HS^- + 2O_2 \rightarrow S_2O3^{2-} + H_2O \quad (1)$$

$$S^0 + 1.5O_2 + H_2O \rightarrow SO_4{}^{2-} + 2H^+ \quad (2)$$

$$S_2O_3{}^{2-} + 2O_2 + H_2O \rightarrow 2SO_4{}^{2-} + 2H^+ \quad (3)$$

$$2H_2 + O_2 \rightarrow 2H_2O \quad (4)$$

$$H_2 + S^0 \rightarrow HS^- + H^+ \quad (5)$$

$$S^0 + 4H_2O \rightarrow SO_4{}^{2-} + 3HS^- + 5H^+ \quad (6)$$

Cells did not grow with $HS^-$ when provided with 2% $O_2$ as electron acceptor (Eq. 1), possibly due to the fast kinetics of abiotic and $O_2$-dependent $HS^-$ oxidation at circumneutral pH[64,65], as further discussed below. When cells were provided with $S^0$ or $S_2O_3^{2-}$ as the electron donor and 2% $O_2$ as the electron acceptor (Eqs. 2 and 3), the concentration of cells increased concomitant with an increase in the concentration of $SO_4^{2-}$ (Supplementary Fig. 4). When *Hydrogenobacter* RSW1 was provided with $H_2$ as an electron donor and 2% or 5% $O_2$ as the electron acceptor (Eq. 4), cell concentrations also increased (Fig. 3B). When cultures were provided with $H_2$ as the electron donor and $S^0$ as the electron acceptor (Eq. 5), the concentration of $HS^-$ increased but no change in the cell concentration was observed (Fig. 3A, B). $HS^-$ concentrations were below the detection limit (<1 μM; Supplementary Fig. 5) in abiotic controls, indicating that $HS^-$ measured in biologic experiments is biogenic. This suggests that the $H_2/S^0$ redox couple may support the energy metabolism of the cell but that this is not coupled to biomass production (discussed below). This observation is consistent with prior characterization of the Aquificales bacteria *T. ruber* and *A. aeolicus*, which were also shown to be capable of reducing $S^0$[28,40]. In the subsections below, experiments are presented that are aimed at identifying the specific effects of $O_2$ and $H_2$ concentration on

https://doi.org/10.1038/s41467-025-56418-4

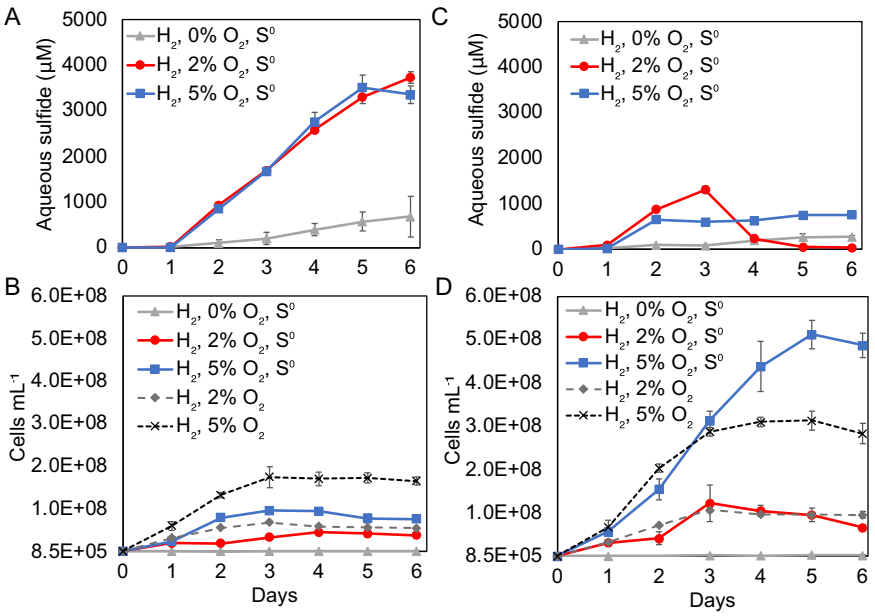


**Fig. 3 | Production of total sulfide and cells in autotrophically grown cultures of *Hydrogenobacter* RSW1 in the presence and absence of added oxygen ($O_2$) with and without daily headspace amendment.** Growth experiments were conducted in cultures provided with hydrogen ($H_2$) as reductant, elemental sulfur ($S^0$) as oxidant, and $O_2$ to specified concentrations at the start of the experiment (**A**, **B**) or with daily amendments to maintain $O_2$ at the specified concentrations (panels **C** & **D**). Cultures containing $H_2$ and $O_2$ without $S^0$ were included for growth comparisons (panels **B** & **D**). Total aqueous sulfide ($H_2S/HS^-/S_2^-$) was determined before and after headspace exchange and thus accounts for its loss during headspace exchange (panel **C**). $SO_4^{2-}$ was not produced in experiments containing $S^0$ (Supplementary Fig. 6). All cultures were provided with 150 μM $SO_4^{2-}$ as a sulfur source and were incubated on their sides at 70 °C on a shaking incubator (50 revolutions per minute). The average and standard deviation of three or four replicate cultures is shown. Source data are provided as a Source Data file.

pathways of $S^0$ oxidation and reduction in RSW1 and their effects on the growth and metabolism of cells.

**Impact of $O_2$ concentration on $S^0$ metabolism without reactor headspace exchange.** A previous study of *T. ruber* and *A. aeolicus* reported $H_2$-dependent reduction of $S^0$ to $HS^-$ (Eq. 5) in the presence of $O_2$[28,40], an interesting observation since $S^0$ reduction is a form of anaerobic respiration in many cells[66]. Robust growth was reported for both *T. ruber* and for *A. aeolicus* cells grown under this condition, however, it is unclear from these studies if cells were simultaneously reducing $O_2$ and $S^0$ (Eqs. 4 and 5) and, if so, whether there was a growth benefit[28,40]. Given that *Hydrogenobacter* RSW1 can oxidize $S^0$ or $H_2$ with $O_2$ (Eqs. 2 and 4) and reduce $S^0$ with $H_2$ (Eq. 5), additional investigations into this phenomenon in RSW1 were undertaken. For the following experiments, the final headspace gas composition for anaerobic growth experiments was (vol./vol.): 80% $H_2$ and 20% $CO_2$. For aerobic growth experiments, the amount of $CO_2$ in the headspace remained constant (20% vol./vol.) but the amount of $O_2$ in the headspace was adjusted as specified, while $H_2$ concentrations were adjusted to balance the $O_2$ concentrations, unless otherwise noted. When provided 0% vol./vol. $O_2$, $S^0$, and $H_2$, a total of ~500 μM of $HS^-$ was produced over the course of the incubation but this was not coupled to production of cells (Fig. 3A, B). However, when cells were provided with 2% and 5% vol./vol. $O_2$, $S^0$, and $H_2$, >3.5 mM of $HS^-$ was produced over the course of the incubation and metabolic activity was coupled to the production of cells (Fig. 3A, B). In cultures provided with 2% vol./vol. $O_2/S^0/H_2$, cell concentrations reached a maximum of $4.54 \times 10^7$ cells $mL^{-1}$ whereas those provided with 5% vol./vol. $O_2/S^0/H_2$ reached a maximum of $9.68 \times 10^7$ cells $mL^{-1}$ (Fig. 3B). Production of $SO_4^{2-}$ was not observed in any of these conditions, indicating that cells were not oxidizing $S^0$ with $O_2$ (Eq. 2) or disproportionating $S^0$ to produce $HS^-$ and $SO_4^{2-}$, per Eq. 6 (Supplementary Fig. 6). One hundred fifty μM $SO_4^{2-}$ was provided to all reactors as a sulfur source, such as to not induce cells to metabolize $S^0$ to make it available for assimilation. Cells provided with $H_2$ and 2% and 5% vol./vol. $O_2$ without $S^0$ (Eq. 4) were included for comparison and these reached final concentrations of $6.87 \times 10^7$ cells $mL^{-1}$ and $1.75 \times 10^8$ cells $mL^{-1}$, respectively (Fig. 3B). $HS^-$ was not detected in these conditions. Based on these data, it was hypothesized that $H_2$-oxidizing cells were simultaneously reducing $S^0$ and $O_2$ (Eqs. 4 and 5) to support their energy metabolism, with those cells provided with higher concentrations of $O_2$ gaining additional energy from a greater availability of this oxidant. The aforementioned experiments were performed without headspace exchange, however, which may have allowed for $O_2$ limitation to develop during the course of incubation, leading to a subsequent metabolic switch to $S^0$ reduction.

**Impact of $O_2$ concentration on $S^0$ metabolism with reactor headspace exchange.** The low solubility[67] and the low diffusivity of $O_2$ at high temperature[68] could cause anoxic conditions to develop in cultures that would promote $S^0$ reduction and lead to the erroneous conclusion that the same cells were simultaneously reducing $O_2$ and $S^0$. To begin to rule out this possibility, the same experimental conditions were used as above, however, the headspace of each reactor was flushed for 30 sec followed by replacement of the gas phase to the specified initial concentrations (0%, 2%, or 5% vol./vol. $O_2$) every 24 h during incubation (Fig. 3C, D).

As in the previous experiment, cultures provided with $H_2$ and $S^0$ but not with $O_2$ (0% vol./vol.; Eq. 5) produced $HS^-$ without an increase in cell concentration (Fig. 3C, D). Despite exchanging the headspace every 24 h, cultures provided with 2% or 5% vol./vol. $O_2$, $H_2$, and $S^0$ still produced $HS^-$, generating 1.3 mM $HS^-$ and 715 μM $HS^-$, respectively (Fig. 3C). These concentrations are lower than those measured in non-exchange experiments (Fig. 3A) for reasons discussed below. Both the 2% vol./vol. $O_2/S^0/H_2$ condition and 5% vol./vol. $O_2/S^0/H_2$ condition reached significantly higher cell concentrations, $1.05 \times 10^8$ and $5.13 \times 10^8$ cells $mL^{-1}$, respectively, when compared to the same conditions when the headspace was not exchanged (Fig. 3B, D). This indicates that $O_2$ limitation may have occurred in cultures during the

https://doi.org/10.1038/s41467-025-56418-4

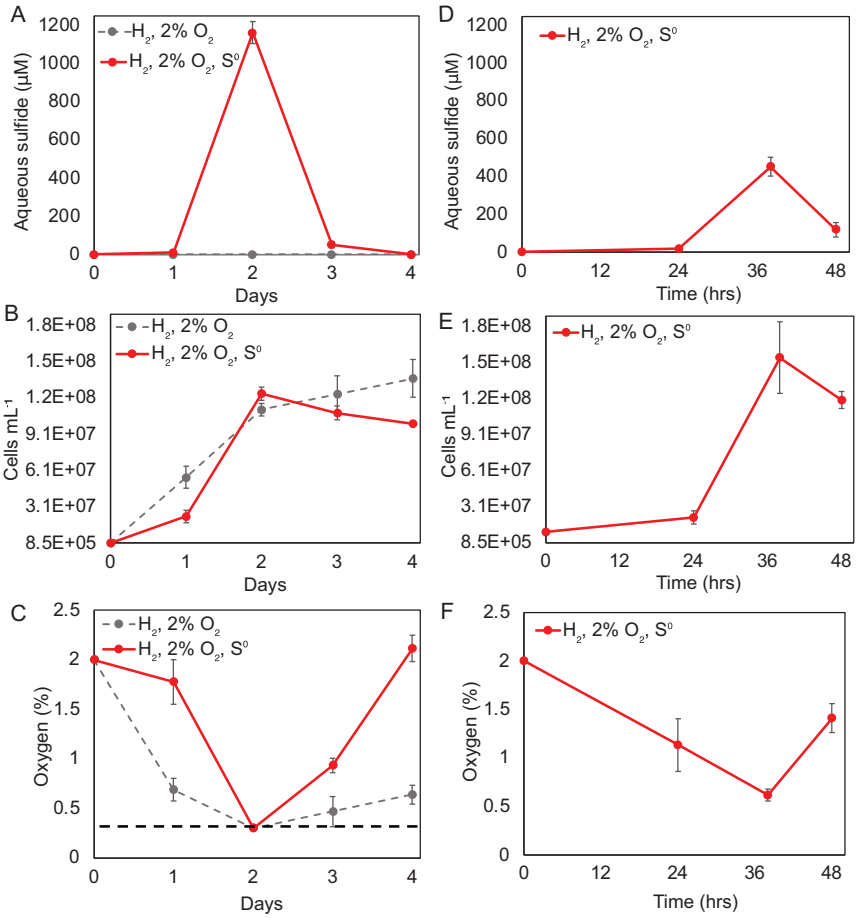


**Fig. 4 | Production of total sulfide, cells, and consumption of oxygen ($O_2$) in autotrophically grown cultures of *Hydrogenobacter* RSW1 in the presence and absence of elemental sulfur ($S^0$).** Growth experiments were conducted in cultures provided with hydrogen ($H_2$) and 2% $O_2$ or with $H_2$, 2% $O_2$ and $S^0$ with daily amendments to maintain $O_2$ at the specified concentrations (**A**–**C**) or with more frequent exchange between 24–48 h (**D**–**F**). Total aqueous sulfide ($H_2S/HS^-/S_2^-$) was determined before and after headspace exchange and thus accounts for its loss during headspace exchange (panels A and D). $O_2$ measurements were taken prior to headspace adjustments (C and F). Dashed line in panel C represents the limit of detection. $SO_4^{2-}$ was not produced in experiments containing $S^0$ (Supplementary Fig. 8). All cultures were provided with ~150 μM $SO_4^{2-}$ as a sulfur source and were incubated on their sides at 70 °C on a shaking incubator (50 revolutions per minute). The average and standard deviation of four replicate (A–C) and three replicate (panels D–F) cultures is shown. Source data are provided as a Source Data file.

course of the experiments without headspace exchange. Although cells provided with $H_2$ and 2% and 5% vol./vol $O_2$ without $S^0$ (Eq. 4) also reached a higher final cell concentration ($1.07 \times 10^8$ cells $mL^{-1}$ and $3.14 \times 10^8$ cells $mL^{-1}$, respectively) when compared to the no headspace exchange experiment, the increase was not as significant as the increase observed in cultures provided with $S^0$ (Fig. 3B, D). Cultures provided with $H_2$ and 2% $O_2$ with and without $S^0$ (Eq. 4) grew similarly when the atmosphere was exchanged, while cultures provided with $H_2$ and 5% $O_2$ in the presence of $S^0$ grew significantly better than cultures provided with $H_2$ and 5% $O_2$ without $S^0$ (Fig. 3D). This indicates that there is a significant growth benefit when $H_2$-oxidizing cells are provided with both $O_2$ and $S^0$.

The lack of stimulation of growth in the 2% $O_2$ condition with $S^0$ is likely explained by the abiotic consumption of $O_2$ by $HS^-$ (discussed below), which may have decreased $O_2$ availability during the course of the incubation, when compared to the condition without $S^0$ (Eq. 4). Further, the amount of $HS^-$ that accumulated in cultures during the course of incubation was not constant, and periods of $HS^-$ accumulation were observed followed by periods of $HS^-$ drawdown towards the end of incubation (Fig. 3C). For example, a substantial amount of $HS^-$ was produced until day three in the 2% $O_2/S^0/H_2$ growth condition but then rapidly disappeared between day three and four. The depletion of $HS^-$ corresponds to a cessation in cell production, suggesting that the decrease was due to inactivity of cells (Fig. 3C-D). $HS^-$ is readily oxidized by $O_2$ at circumneutral pH[64,65], suggesting that the decrease could be attributed to abiotic oxidation. It is unlikely that *Hydrogenobacter* RSW1 is responsible for the decrease in $HS^-$ considering that experiments failed to demonstrate this capability in this strain (Eq. 1; see above). Rather, abiotic control experiments indicated that the $Ni^{2+}$ and $Co^{2+}$ ions (and to a lesser extent $Fe^{2+}$ ions) present in the SL-10 trace metals used to cultivate *Hydrogenobacter* RSW1 catalyzed the oxidation of $HS^-$ and that this required and consumed $O_2$ (see Supplementary Results in the Supplemental Material file, Supplementary Fig. 7).

To further investigate whether anaerobic conditions developed in reactors resulting in $H_2$-oxidizing cells switching from $O_2$ reduction (Eq. 4) to $S^0$ reduction (Eq. 5), as opposed to simultaneous reduction of $O_2$ and $S^0$ (Eqs. 4 and 5), growth experiments containing 2% $O_2$ with or without $S^0$ (Fig. 3C, D) were repeated and headspace $O_2$ concentrations were determined every 24 h prior to replacing the headspace with $H_2/CO_2/O_2$ to specified concentrations. $HS^-$ and/or cell production in both growth conditions (Fig. 4A, B) were similar to what was measured previously (Fig. 3C, D). In both culture conditions, the concentration of $O_2$ in the headspace decreased during the incubation period (Fig. 4C). In the $H_2/O_2$ condition (Eq. 4), the rate of $O_2$ consumption was faster than in the $H_2/O_2/S^0$ condition, which was reflected in the production of more cells in the former condition relative to the latter condition between days 0 and 1. The slower rate of cell production when $S^0$ was present indicates that $S^0$ affects the coupling of $H_2$ oxidation to $O_2$

https://doi.org/10.1038/s41467-025-56418-4

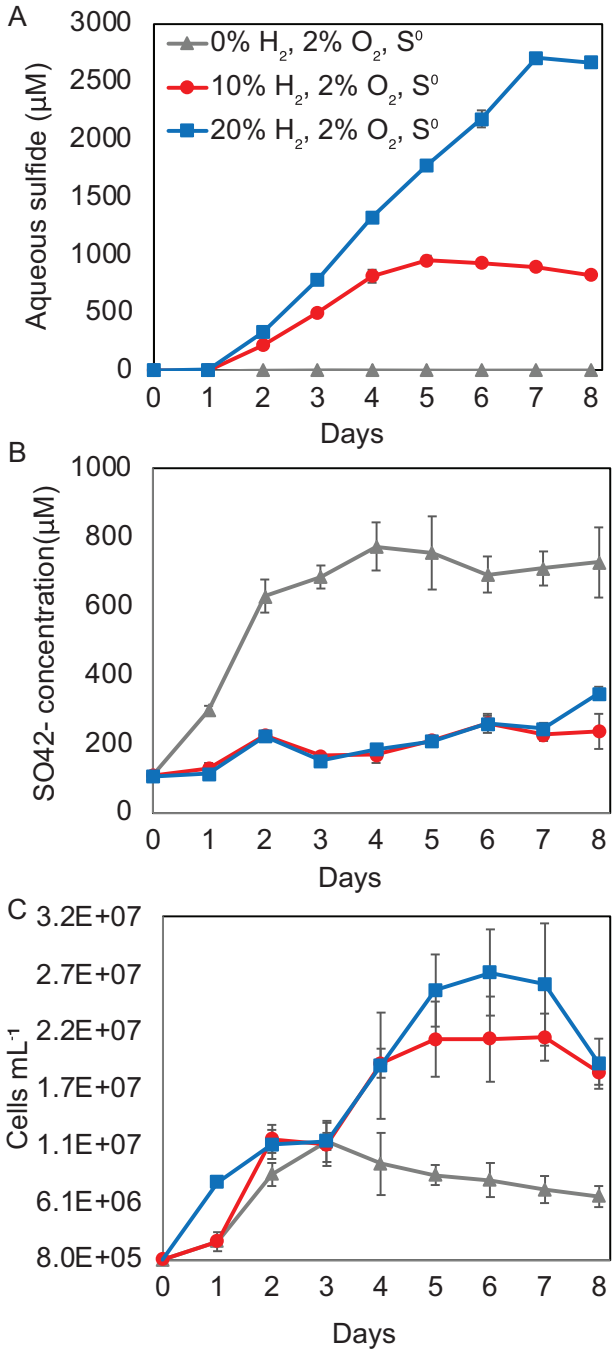


**Fig. 5 | Production of total sulfide, sulfate, and cells under variable hydrogen ($H_2$) concentrations and 2% oxygen ($O_2$) in autotrophically grown cultures of *Hydrogenobacter* RSW1.** Total sulfide ($H_2S/HS^-/S^{2-}$; panel **A**) concentration, sulfate ($SO_4^{2-}$; panel **B**) concentration, and cell concentration (panel **C**) were measured in cultures provided with $S^0$ and 2% vol./vol. $O_2$ in the headspace with specified amounts of $H_2$ (vol./vol. in headspace). All cultures were provided with 150 μM $SO_4^{2-}$ as a sulfur source and cultures were incubated on their sides at 70 °C on a shaking incubator (50 revolutions per minute). The average and standard deviation of triplicate cultures is indicated. Source data are provided as a Source Data file.

reduction. Alternatively, the inoculum for this experiment was $H_2/O_2$-grown cells, which may have led to the longer lag in $H_2/O_2/S^0$-grown cultures. Between days 1 and 2, nearly 1.2 mM of $HS^-$ was produced in $H_2/O_2/S^0$-grown cultures, which is attributable to $S^0$ reduction, and the rate of cell production was faster than in $H_2/O_2$-grown cultures. In both growth conditions, $O_2$ concentrations were depleted from 2% to <0.3% (limit of detection) between 1 and 2 days of incubation (Fig. 4C). No increase in $SO_4^{2-}$ concentration was detected in these conditions (Supplementary Fig. 8), indicating that these cells are not growing via $S^0$ oxidation (Eq. 2) or through the disproportionation of $S^0$ (Eq. 6). This shows that $O_2$ likely became limiting and the presence of $S^0$ allowed for additional $H_2$ oxidation and growth. However, these data do not indicate that $O_2$ was depleted before $S^0$ reduction occurred.

To determine if $HS^-$ production in $H_2/O_2/S^0$ conditions is due to depletion of $O_2$ through $H_2$ oxidation (Eq. 4) followed by the reduction of $S^0$ (Eq. 5) or whether reduction of substrates occurs simultaneously, the same experiment with 2% $O_2$, $S^0$, and $H_2$ described above was initiated, but with the headspace being exchanged more frequently at 24, 38, and 48 h (Fig. 4D–F). The rates of cell production and $O_2$ consumption were similar to previous experiments, although only 400 μM of $HS^-$ accumulated (Fig. 4D). This is attributable to the higher concentration and total amount of $O_2$ in these experiments. Importantly, the concentration of $O_2$ decreased in the headspace as cell and $HS^-$ concentrations increased (Fig. 4E, F). Together, these data indicate that *Hydrogenobacter* RSW1 simultaneously catalyzed the $H_2$-dependent reduction of $S^0$ and $O_2$ (via Eqs. 4 and 5). It is suggested that this hybrid aerobic-anaerobic metabolism may have been overlooked in Aquificales (and possibly other microorganisms) in previous studies due to efficient abiotic oxidation of $HS^-$ by trace elements in the growth medium used to cultivate cells.

**Impact of $H_2$ concentration on $S^0$ metabolism.** To better understand $S^0$ reduction activity in cultures of *Hydrogenobacter* RSW1, experiments were established to vary $H_2$ concentrations in cultures while keeping $O_2$ concentrations constant. Headspace $H_2$ concentrations of 0%, 10% and 20% vol./vol. were tested while keeping the headspace $O_2$ concentration at 2% vol./vol. All experiments contained the same amount of $S^0$ and had a $N_2$ headspace with 20% $CO_2$ that was amended with $H_2$ and $O_2$ to meet the target concentrations. When given 0% $H_2$, 2% $O_2$, and $S^0$, $HS^-$ was not detected (Fig. 5A), while nearly 700 μM of $SO_4^{2-}$ was produced (Fig. 5B), indicating $S^0$ oxidation activity (Eq. 2). In this growth condition, the cell concentration increased from $8.0 \times 10^5$ cells $mL^{-1}$ to $1.1 \times 10^7$ cells $mL^{-1}$ (Fig. 5C). In contrast, cultures provided with 10% or 20% $H_2$, 2% $O_2$, and $S^0$, produced roughly 1 mM and 2.5 mM of $HS^-$, respectively (Fig. 5A), with minimal increases in $SO_4^{2-}$ (~150 μM) (Fig. 5B). Cell concentrations increased from $8.27 \times 10^5$ cells $mL^{-1}$ to $2.13 \times 10^7$ cells $mL^{-1}$ at 10% $H_2$ and from $7.91 \times 10^5$ cells $mL^{-1}$ to $2.73 \times 10^7$ cells $mL^{-1}$ at 20% $H_2$ (Fig. 5C). The maximum cell concentrations in the $H_2$-containing growth experiments were significantly higher than in those conducted in the absence of $H_2$ (Fig. 5C). Despite minimal increases in $SO_4^{2-}$ (~150 to 200 μM over 8 days incubation) measured in the 10% and 20% vol./vol. $H_2$, $S^0$, and 2% vol./vol. $O_2$ conditions, the amount produced cannot explain the increase in cell production and is non-stoichiometric with the amount of $HS^-$ produced that would be predicted for $S^0$ disproportionation (Eq.6; 3 $HS^-$ to 1 $SO_4^{2-}$), consistent with the lack of known disproportionating enzymes encoded in the RSW1 genome. These data indicate that $H_2$ stimulated activity in the presence of $S^0$ and $O_2$ and further suggests that cells were simultaneously reducing $S^0$ and $O_2$ with $H_2$, as discussed above. It is also possible that cells were also oxidizing $S^0$ (Eq. 2), albeit at a minimal level. If true, this would indicate that simultaneous reduction of $S^0$ and $O_2$ is occurring during simultaneous oxidation of $H_2$ and $S^0$, adding further to the metabolic complexity of RSW1.

**Combined Impact of $H_2$ and $O_2$ concentrations on $S^0$ metabolism.** To begin to bracket the concentrations of $O_2$ and $H_2$ that dictate the mode or directionality of $S^0$ metabolism in *Hydrogenobacter* RSW1, cultures were provided with $S^0$, 5% vol./vol. $O_2$, and $H_2$ at headspace concentrations of 0%, 10%, and 20% vol./vol. At 0% and 10% vol/vol. $H_2$, $HS^-$ was not detected while over 1 mM of $SO_4^{2-}$ was produced in both conditions (Supplementary Fig. 9A, B). In these growth conditions, the concentration of cells increased from 1.19 $\times 10^6$ and $1.27 \times 10^6$ to

https://doi.org/10.1038/s41467-025-56418-4

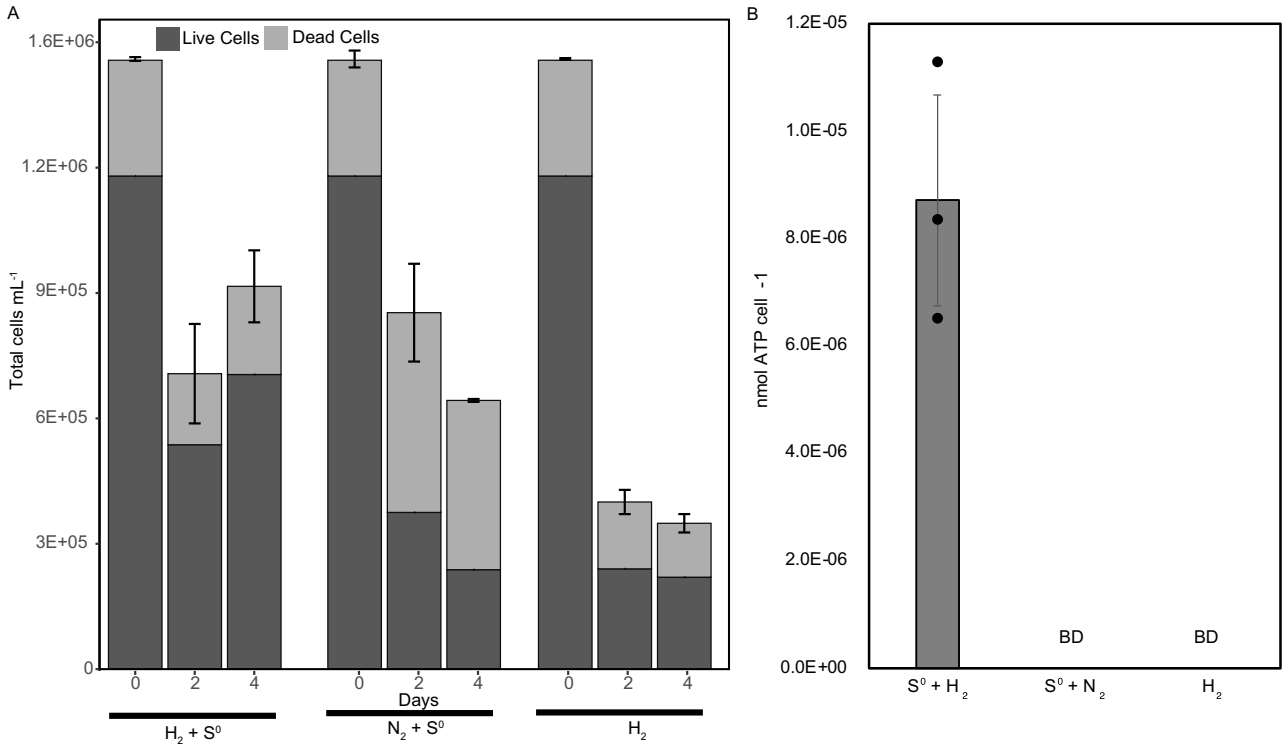


**Fig. 6 | Viability and ATP content of *Hydrogenobacter* RSW1 cells when incubated in the presence and absence of an electron donor ($H_2$) or an electron acceptor ($S^0$).** Cell concentration and cell viability (panel **A**) were quantified in cultures grown with hydrogen ($H_2$) and elemental sulfur ($S^0$), with $S^0$ only, or with $H_2$ only over 4 days of incubation. The production of cells and their viability was determined using live/dead staining and fluorescent microscopy (panel **A**). ATP content of cells following 4 days of incubation as determined using a firefly luciferase assay (panel **B**). Individual replicates are shown as black circles. All cultures were provided with 150 μM $SO_4^{2-}$ as a sulfur source and were incubated on their sides at 70 °C on a shaking incubator (50 revolutions per minute). The average and standard deviation of measurements of triplicate cultures is indicated. Abbreviations: BD, below detection. Source data are provided as a Source Data file.

$2.13 \times 10^7$ and $6.42 \times 10^7$ cells $mL^{-1}$, respectively, indicating that cells are coupling aerobic oxidation of $S^0$, per Eq. 2, to growth (Supplementary Fig. 9C). It is not known if the cells are also oxidizing $H_2$ in these conditions (Eq. 4), although the higher cell concentration reached when $H_2$ is present suggests that $H_2$ stimulated growth even when cells were oxidizing $S^0$. In contrast, in cultures grown with $S^0$, 20% vol/vol. $H_2$ and 5% vol/vol. $O_2$, a total of ~550 μM of $HS^-$ was produced while no significant increase in $SO_4^{2-}$ was detected (Supplementary Fig. 9A, B). The concentration of cells increased from $1.24 \times 10^6$ to $1.23 \times 10^8$ cells $mL^{-1}$ in this growth condition (Supplementary Fig. 9C). The production of $HS^-$ and cells without production of $SO_4^{2-}$ indicates that $H_2$ oxidation is being coupled to the simultaneous reduction of $S^0$ and $O_2$ (Eqs. 4 and 5). Collectively these data indicate that the availability of both $O_2$ and $H_2$ impact the mode of $S^0$ metabolism in RSW1. At 10% $H_2$, the mode of $S^0$ metabolism by cultures of RSW1 is dependent on the concentration of $O_2$, whereby cells reduced $S^0$ at ≤2% $O_2$ but oxidize $S^0$ at ≥5% $O_2$. In contrast, at 20% $H_2$, cultures of RSW1 reduced $S^0$ regardless of the $O_2$ concentration (Fig. 5, Supplementary Fig. 9). These data also suggest that regardless of whether cells are oxidizing or reducing $S^0$, the presence of $H_2$ has a stimulatory effect on growth of cells, resulting in higher cell concentrations when incubations contain any amount of $H_2$ (Fig. 5, Supplementary Fig. 9).

**Cell Viability and ATP production in $H_2/S^0$ reducing cells.** To determine whether anaerobic $S^0$ reduction provides cells a benefit despite a lack of increase in cell concentration, live/dead staining was used to examine the viability of cells under three different conditions: $H_2/S^0$, $N_2/S^0$, and $H_2$ only. After four days of incubation at 70 °C, the total number of cells and those that were deemed viable via live/dead staining differed markedly under the various growth conditions. The total number of cells decreased by $5.44 \times 10^5$ cells $mL^{-1}$ (37%), $8.17 \times 10^5$ cells $mL^{-1}$ (56%), and $1.11 \times 10^6$ cells $mL^{-1}$ (76%) following four days incubation in the presence of $H_2/S^0$, $N_2/S^0$, or $H_2$ only (Fig. 6A). Of the total cells remaining after four days of incubation, cells that remained viable decreased by $4.77 \times 10^5$ cells $mL^{-1}$ (40%), $9.46 \times 10^5$ cells $mL^{-1}$ (80%), and $9.63 \times 10^5$ cells $mL^{-1}$ (81%) in $H_2/S^0$, $N_2/S^0$, or $H_2$ respectively (Fig. 6A). Together, these data indicate that cells provided with the $H_2$ and $S^0$ have a clear advantage over the other conditions, with the highest percentage of live cells remaining after four days of incubation. This indicates that the $H_2/S^0$ redox couple is providing a physiological benefit to cells in the absence of $O_2$.

Given the membrane-associated nature of the Hyd-Sre complex (Fig. 2), it is possible that the metabolism of the $H_2$ and $S^0$ couple allows for the generation of an electrochemical potential that can be used to drive ATP synthesis. While experiments were not done to directly measure the electrochemical potential in cells grown with $H_2/S^0$, $N_2/S^0$, or $H_2$ only, an experiment was performed to quantify the concentration of ATP in cells following four days of incubation at 70 °C. The only cells that had detectable ATP above background values were those provided with $H_2$ and $S^0$ (Fig. 6B). It should be noted that RSW1 cells were difficult to lyse, and the ATP measurements reported herein should be regarded as qualitative. Nonetheless, the production of ATP in cultures provided with $H_2$ and $S^0$ and the lack of detectable ATP in the other growth conditions suggests that RSW1 can respire $S^0$ with $H_2$. Why the $H_2/S^0$ redox couple cannot support growth is not clear given that it can support growth in other cells. Nevertheless, the $H_2/S^0$ redox couple clearly provides an energetic benefit to the cells, both in the presence and absence of $O_2$.

https://doi.org/10.1038/s41467-025-56418-4

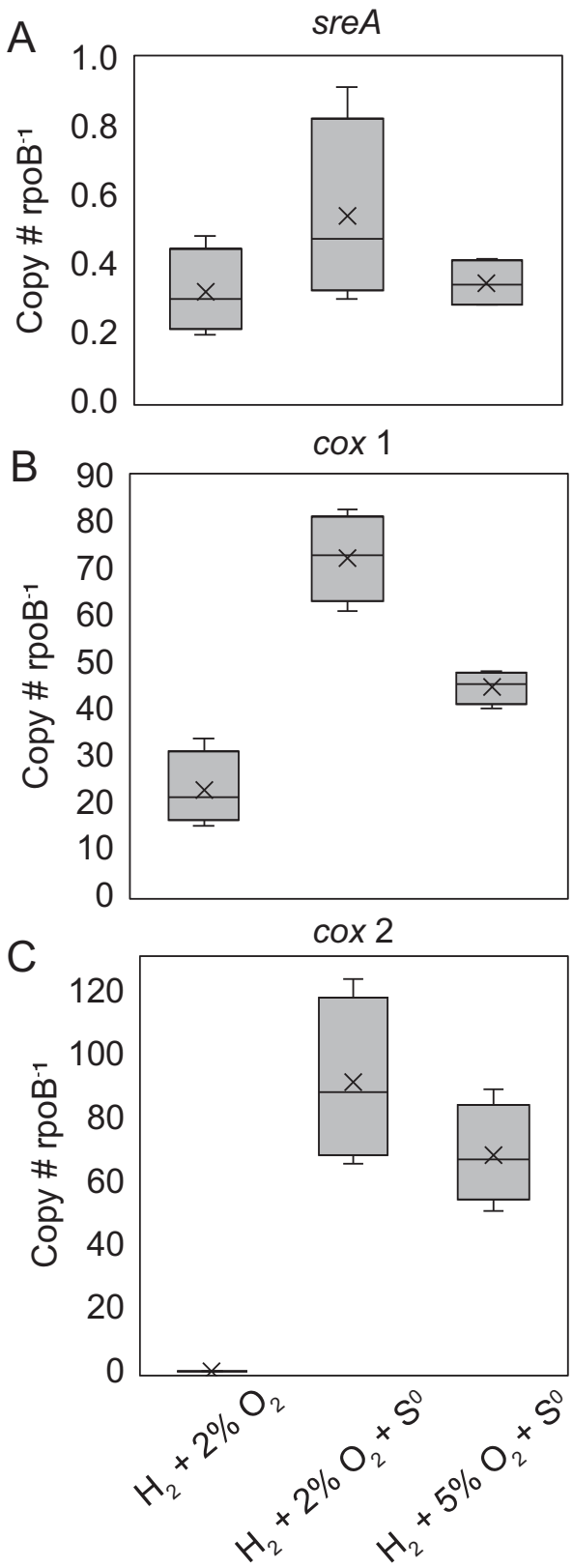


**Fig. 7 | Transcriptional regulation of genes encoding proteins hypothesized to be involved in sulfur respiration ($S^0$), and oxygen ($O_2$) respiration, as determined by quantitative PCR on reverse transcribed complementary DNA (cDNA).** Panels **A**-**C** depict the expression of a single gene of interest normalized to RNA polymerase subunit beta (*rpoB*) transcript copy number for each condition tested. All cultures were provided with 150 µM $SO_4^{2-}$ as a sulfur source and were incubated on their sides at 70 °C on a shaking incubator (50 revolutions per minute). Cultures were harvested at mid-log phase for RNA extraction and subsequent conversion to cDNA. Data from four replicate cultures are plotted. Box plots show the upper quartile, lower quartile, mean (represented by x), and the median (represented by the solid line). Whiskers represent the maximum and minimum value. There are no outliers in the dataset. Source data are provided as a Source Data file.

**Transcriptional regulation of $S^0$ and $O_2$ metabolism in RSW1.** The apparent simultaneous $H_2$-dependent respiration of $S^0$ and $O_2$ by *Hydrogenobacter* RSW1 suggests complex regulation of *sre* and/or *cox* used to metabolize $S^0$ and $O_2$, respectively. To begin to investigate the transcriptional regulation of genes involved in these processes, primers were designed for genes of interest (GOI), including the alpha subunit of sulfur reductase (*sreA*) and two isoforms of subunit 1 of cytochrome *c* oxidase (*cox*1 and *cox*2). Autotrophically grown cells were cultivated under three different conditions ($H_2 + O_2$; $H_2$ + 2% $O_2 + S^0$, and $H_2$ + 5% $O_2 + S^0$) with headspace exchange to prevent $O_2$ limitation (Fig. 3C, D. Fig. 4). RNA was not recovered from cultures provided with $H_2/S^0$ only, preventing a comparison of expression patterns under this growth condition.

Interestingly, expression of *sreA* varied only slightly among the conditions and was not upregulated in any conditions compared to *rpoB* (Fig. 7A), suggesting constitutive expression of *sre* or possible post-transcriptional regulation. *sre* and *hyd*1 are not spatially co-localized in the genome despite being hypothesized to encode proteins that form a membrane-associated complex[40,59]. This may indicate a lower likelihood that these genes are co-regulated, as opposed to genes that are proximal on the genome. Both *cox*1 and *cox*2 were upregulated in both the $S^0/H_2/2\%O_2$ and the $S^0/H_2/5\%O_2$ relative to the $H_2$/2% $O_2$ condition (Fig. 7B, C). In many bacteria, expression of multiple isoforms of *cox* is regulated by availability of $O_2$[69]. Cells were harvested for RNA during mid log phase, at around 44 h (20 h after the first headspace exchange). Based on growth and activity data presented above (Fig. 4A–C), it is likely that $O_2$ had become limiting in 2% $O_2/H_2$ cultures not provided with $S^0$ but was still available in cultures that were provided with 2% $O_2/H_2/S^0$ or 5% $O_2/H_2/S^0$. As such $O_2$ limitation could explain the down-regulation of *cox* in the $H_2/O_2$ condition. Nonetheless, co-expression of both *sre* and *cox* in cultures grown with $H_2/S^0/O_2$ supports the conclusion that RSW1 simultaneously respires aerobically and anaerobically through the simultaneous reduction of $S^0$ and $O_2$.

## Implications

Data presented here suggests that a strain of *Hydrogenobacter* (RSW1) isolated from a circumneutral hot spring in YNP sourced by the anoxic deep hydrothermal aquifer is capable of simultaneously respiring aerobically and anaerobically by reducing $O_2$ and $S^0$ with $H_2$ as reductant. Although RSW1 could not couple $H_2$-dependent anaerobic $S^0$ reduction to growth, cells produced $HS^-$ in this condition and had higher viability and ATP levels. This indicates that the $H_2/S^0$ redox couple is used to generate an electrochemical gradient to power ATP synthesis and thus would represent a selectable fitness advantage in the presence or absence of available $O_2$. These data help to reconcile previous observations in *T. ruber* and *A. aeolicus* that indicated $HS^-$ production from $S^0$ in aerobically grown cultures[28,40]. The distribution of Sre is widespread among members of the Aquificales, other Bacteria, and some Archaea[59], with 100% of the *Thermocrinis* genomes, 50% of the *Hydrogenobacter* genomes, and all *Hydrogenivirga* genomes (all members of the Aquificaceae) encoding homologs of SreA. This suggests the possibility that this hybrid mode of energy metabolism may extend beyond RSW1, *T. ruber*, and *A. aeolicus* to other members of this order and potentially to other organisms encoding Sre. Further, it should be noted that $HS^-$ cycling with $O_2$ and trace metals led to rapid oxidation of $HS^-$ in cultures grown under optimal, laboratory

conditions. In natural environments where growth conditions are typically suboptimal, it is possible that $HS^-$ may not accumulate due to quick and efficient abiotic oxidation by trace metals/$O_2$ in what has been referred to as the cryptic sulfur cycle[70,71]. Given that trace elements such as Ni and Co can be enriched in hot springs[72], it is possible that this metabolism could easily be overlooked in these environments due to rapid oxidation of $HS^-$.

A hybrid energy metabolism like that described herein for RSW1 (and extended to *T. ruber*, *A. aeolicus*, and possibly other organisms) could be ecologically beneficial to cells that inhabit environments where the supply of oxidants are limited and/or highly variable. The delivery of $O_2$ to hot springs sourced by deep, anoxic fluids is primarily through atmospheric ingassing, which is likely to be limited and variable depending on the amount of turbulence created by gas efflux and the temperature of the spring. Such conditions might select for cells that can maintain an electrochemical potential by respiring lower potential oxidants, such as $S^0$, when higher potential oxidants, such as $O_2$, are temporally not available. For reasons that are not clear, respiration of $S^0$ is not coupled to growth in RSW1. However, when $O_2$ is available, RSW1 continues to respire $S^0$ while respiring $O_2$. Together, these activities would provide additional energy to drive biomass synthesis. This could explain the apparent constitutive expression of *sre* and upregulation of *cox*1 and *cox*2 in cells provided with both $S^0$ and 2% or 5% $O_2$ relative to cells only provided with 2% $O_2$ which likely became limiting. In this model, $S^0$ reduction allows for ATP to be generated to maintain cell viability during periods of anoxia.

Aquificales are often considered to be among the earliest diverging thermophilic Bacteria[47,73], with those that are obligate anaerobes (Desulfurobacteriaceae) diverging earlier than obligate microaerophiles (Hydrogenothermaceae, Aquificaceae) (Fig. 1). Observations made here could provide insight into a strategy that enabled anaerobic bacteria to diversify to take advantage of $O_2$ as it became progressively more available. While current paradigms suggest that facultatively anaerobic organisms shift from anaerobic to aerobic respiration when $O_2$ is available to maximize energy gain and to not toxify anaerobic biochemistry, it is possible that the ephemeral nature of $O_2$ in modern hot springs remains reminiscent of early Earth when whiffs of $O_2$ began to enter the biosphere[74] and continues to select for organisms adapted to such conditions. It could be a selective disadvantage to cells to wholly shift to aerobic energy metabolism if the bioenergetic costs of such a metabolic shift (i.e., synthesizing new proteins) outweighs the energy gain. Alternatively, it is possible that Sre was acquired after the rise in $O_2$ occurred and has been maintained due to the selective advantage it provides. While simultaneous anaerobic and aerobic respiration has not been suggested or identified prior to this study, this observation is not inconsistent with reports of anaerobic metabolisms (e.g., $SO_4^{2-}$ reduction) occurring in the presence of $O_2$ (e.g.,[75–77]) and could be a significant oversight in the current understanding of microbial metabolisms. As such, this metabolic strategy has the potential to be widespread among organisms living in dynamic environments, such as hot springs, intertidal zones, and microbial mats due to the selective advantage that it provides for such organisms.

## Methods

### Sample collection, enrichment, and isolation

Roadside West (RSW; N 44°45'12.7"; W 110°43'40.1") is in the Nymph Lake area along the Norris-Mammoth Corridor, Wyoming, U.S.A (Supplementary Fig. 1). Field determinations of hot spring pH and temperature were made using a WTW combination pH probe (Weilheim, Germany) and conductivity was measured using a temperature-compensated YSI meter (YSI Inc., Yellow Springs, OH). Dissolved oxygen (DO) concentrations were measured on-site using a high-temperature PSt3 oxygen dipping probe and a Fibox 4 DO instrument (PreSens, Regensburg, Germany). Total sulfide ($H_2S/HS^-/S_2^-$ and acid volatile sulfide; herein termed $HS^-$ since this is the most prevalent form at pH 7.0[67]) and ferrous iron (Fe(II)) concentrations in hot spring waters were quantified in the field within a minute of sample collection using Hach sulfide reagents 1 and 2, Hach ferrozine pillows, and a Hach DR/890 field deployable spectrophotometer (Hach Company, Loveland, CO). Waters were not filtered prior to determination of $HS^-$ or Fe(II). Water for determination of sulfate ($SO_4^{2-}$) and chloride ($Cl^-$) was filtered (0.22 μm) into polypropylene bottles and stored at 4 °C. Upon arrival at the lab, Hach $SO_4^{2-}$ and $Cl^-$ test kits and the Hach DR/890 field deployable spectrophotometer were used to determine concentrations of $SO_4^{2-}$ and $Cl^-$. Dissolved gas concentrations and additional geochemical analyses of RSW spring water are reported previously[43,44].

Roughly 1 g of flocculant sediment from RSW (pH 6.8, 68°C) was collected on June 21, 2017. The sample was collected aseptically using a flame sterilized spatula, transferred to a 70 mL serum bottle, filled with spring water, and capped with a butyl rubber stopper. The slurry was transported back to the lab at ambient temperature ( ~ 21 °C) where it was then used to inoculate enrichment medium. Mineral salts enrichment medium was composed of $NH_4Cl$ (0.33 g $L^{-1}$), $CaCl_2 \cdot 2H_2O$ (0.1 g $L^{-1}$), KCl (0.33 g $L^{-1}$), $MgCl_2 \cdot 6H_2O$ (0.33 g $L^{-1}$), $Na_2SO_4 \cdot 10H_2O$ (0.03 g $L^{-1}$), $K_2HPO_4$ (0.1 g $L^{-1}$), and Tris-HCl (1.0 g $L^{-1}$), with the pH adjusted to 7.0 using NaOH. All glassware was soaked in trace metal grade 10% nitric acid (10% vol./vol. in MilliQ water) overnight and then rinsed in MilliQ water prior to use in experiments. Fifty-five mL of media was dispensed into 165 mL serum bottles, and these were capped and sealed prior to autoclave sterilization. After autoclaving and while serum bottles were still hot, medium was purged for 20 min with $N_2$ passed over heated (250 °C) and hydrogen ($H_2$)-reduced copper shavings. Unless stated otherwise, the headspace (110 mL) of serum bottles was then adjusted to a final composition of (vol./vol.): 78% $H_2$, 20% carbon dioxide ($CO_2$), and 2% oxygen ($O_2$). Anoxic and filter-sterilized solutions of SL-10 trace metals[78] and Wolfe's Vitamins[79] were added using $N_2$-flushed syringes and needles to final concentrations of 2 mL $L^{-1}$. A serial dilution (ten-fold) enrichment experiment was conducted using 5.0 mL of the sediment-spring water slurry as the initial inoculum. Enrichment progress was monitored by enumeration of cells. Briefly, 2 μL of 4',6-diamidino-2-phenylindole (DAPI; 2 μg/mL final concentration) was added to sub-samples of culture that were then incubated at room temperature ( ~ 21 °C) for 15 min. Samples were then treated with detergent [100 mM ethylenediaminetetraacetic acid (EDTA), 100 mM sodium pyrophosphate, 1% (v/v) Tween 80] to disaggregate cells[80]. Disaggregated and stained cells were filtered onto black polycarbonate filters (0.22 μm) (Millipore, Billerica, MA) and were enumerated using an Evos fluorescent microscope (Life Technologies, Carlsbad, CA). After several transfers of the most dilute enrichment culture, a single morphotype was observed via fluorescence microscopy.

### DNA extraction, genome sequencing

Ten milliliters of a log phase culture exhibiting a single morphotype were subjected to centrifugation (4696 x *g*, 30 min, 4 °C) to pellet cells. DNA was extracted from the pelleted biomass with the MP Bio FastDNA spin kit (MP Biomedicals, Irvine, CA) following manufacturer guidelines and DNA was quantified using the Qubit dsDNA high sensitivity assay kit (Invitrogen, Waltham, MA). Genomic DNA underwent library preparation and was sequenced by the University of Wisconsin Biotechnology Center Sequencing Facility using the Illumina NovaSeq6000 platform. Reads were trimmed and down sampled using TrimGalore v.0.6.0 (https://github.com/FelixKrueger/TrimGalore) and BBMap (https://sourceforge.net/projects/bbmap/). Trimmed and down sampled reads were then assembled using Spades v.3.14.0[81] with default parameters. Proteins were predicted and annotated with PROKKA[82] using default parameters. These gene predictions were further evaluated using the Kyoto Encyclopedia of Genes and Genomes (KEGG) database[83] and the KEGG Automatic Annotation Server

(KAAS)[84] to determine potential metabolic pathways and functions encoded by the RSW1 genome. KEGG annotations were further scrutinized manually using National Center for Biotechnological Information (NCBI) BLASTp and alignment tools. Raw reads were analyzed using the SingleM platform (v.0.15.0) and the 'pipe' function with default parameters[45] to confirm that the culture is an isolate. Average nucleotide identity (ANI) and average amino acid identity (AAI) between genomes and encoded proteins was calculated using the ANI and AAI calculation tool[85].

### Phylogenetic distribution of sulfur reductase (Sre) among aquificales genomes

Genomes and MAGs affiliated with the order Aquificales were compiled from the Integrated Microbial Genomes (IMG) and NCBI databases. Additionally, MAGs from sediments collected from 37 hot springs sampled across YNP that vary in temperature and pH[86] were included in the analysis. Accession numbers for all MAGs utilized can be found in Supplementary Fig. 2.The markerfinder script (https://github.com/faylward/markerfinder) was then used to search the genomic data for 30 universal marker genes that were aligned with ClustalO (v.1.2.4)[87] and concatenated. The concatenated alignment was subject to Maximum-Likelihood phylogenetic construction using IQ-Tree[88]. Model finder plus (MFP) was used to determine the best substitution model for the dataset and 1000 'ultrafast' bootstraps were used to determine branch support. Three different species of *Thermotoga* were used to root the tree, and tree was visualized and edited using the Interactive Tree of Life (ITOL)[89] program. The distribution of sulfur reductase subunit alpha (SreA) homologs was determined via BLASTp analysis against each genome or MAG using SreA from *Aquifex aeolicus* (WP_010880782.1;[40]) as a query with e-value cut-off set at $10^{-80}$ and query coverage set to 70.

### Growth conditions and quantification

Mineral salts medium, prepared as described above, was used in all cultivation experiments. The final headspace gas composition for anaerobic growth experiments was (vol./vol.): 80% $H_2$ and 20% $CO_2$. For aerobic growth experiments, the amount of $CO_2$ in the headspace remained constant (20% vol./vol.) but the amount of $O_2$ in the headspace was adjusted as specified, while $H_2$ concentrations were adjusted to balance the $O_2$ concentrations, unless otherwise noted. Serum bottles amended with $S^0$ were prepared using a modified protocol from what is described above to avoid melting the mineral (melting point is ~ 112 °C). Instead of capping bottles prior to autoclaving, bottles were covered with aluminum foil and were autoclaved alongside new butyl rubber stoppers. After autoclaving but while still hot, $S^0$ (baked at 100 °C for 24 h) was added to a final concentration of 5 g $L^{-1}$. Bottles were immediately capped and sealed with autoclaved rubber stoppers and crimp caps, and the medium was immediately purged with filtered $N_2$ as described above. Wolfe's vitamin solution and SL-10 trace metal solution were added prior to inoculating as described above. $HS^-$ and thiosulfate ($S_2O_3^{2-}$) oxidation growth experiments were conducted in an 80/20% vol./vol. $N_2/CO_2$ headspace with 2% vol./vol. $O_2$ and were provided with 500 μM $Na_2S$ as the $HS^-$ source or 1 mM $Na_2S_2O_3$ as the $S_2O_3^{2-}$ source, respectively. All experiments were incubated at 70 °C on their side on a shaking platform incubator (50 rpm) to increase infusion of headspace gases into the medium, unless otherwise noted. The net production of total $HS^-$ during growth was quantified using the methylene blue assay[90] on subsamples of unfiltered culture. $SO_4^{2-}$ concentrations were determined using a turbidimetric assay[91] on subsamples of unfiltered culture. Cell concentration was determined microscopically as described above. $O_2$ concentrations in the headspace were measured via gas chromatography by injecting 0.25 mL of gas into an injector valve set at 125 °C in a Shimadzu GC-2014 gas chromatograph (Shimadzu, Kyoto, Japan) equipped with a 2.0 M x 1/8" Molecular Sieva 5 A 60/80 column (Ohio Valley Specialty Company, Marietta, OH) with the oven temperature set to 40 °C. $O_2$ was measured using a thermal conductivity detector (TCD) set to 150 °C with ultrahighpurity (UHP) argon as the carrier gas. Peak height for samples was converted to percent using a standard curve generated with UHP $O_2$ (EGas Depot, Largo, FL). Abiotic $S^0$ reducing experiments (Supplementary Fig. 5) were prepared as described above, were uninoculated, and were incubated at 70 °C. Methods for abiotic $HS^-$ oxidation experiments (Supplementary Fig. 7) can be found in the Supplemental Materials file.

### Cell viability experiments and ATP assays

Cell viability experiments were conducted by incubating *Hydrogenobacter* RSW1 cells under three different conditions: 1) $H_2 + S^0$, 2) $N_2 + S^0$, or 3) $H_2$ only. Base salts growth medium was prepared as described above. The carbon source in all experiments was $CO_2$ at a final concentration of 20% (vol./vol.) in the headspace. Where indicated, $H_2$ was added to a final concentration of 80% (vol./vol.) in the headspace, $S^0$ was provided to a final concentration of 5 g $L^{-1}$, and $N_2$ was added to a final concentration of 80% (vol./vol.) in the headspace. To determine the viability of cells in each of the three conditions, a LIVE/DEAD stain (Invitrogen, Waltham, MA) was used following manufacturer's protocols. Cells were counted on an EVOs M5000 fluorescent microscope (Life Technologies, Carlsbad, CA) using the overlay function and GFP and Texas Red light cubes (Life Technologies). On the fourth day of incubation, cells were harvested by centrifugation (4696 x *g*, 35 min, 4 °C). Supernatant was discarded and pellets were used for ATP quantification. Briefly, 500 μL of sterile media was added to pellets and they were resuspended by gentle vortexing. Resuspended cells were transferred to Lysis E Matrix bead beating tubes (MP Biomedicals). Five hundred μL of phenol/chloroform (1:1 ratio) was added to each tube and tubes were subjected to ballistic bead beating (Mini-BeadBeater 16, Biospec Products, Bartlesville, OK) for 20 s to promote cell lysis. Tubes containing lysates were then transferred to a pre-cooled centrifuge (4 °C) and were spun for 5 min at 14,000 x *g* (4 °C) to separate the aqueous phase. The upper aqueous phase was transferred to a sterile microcentrifuge tube for ATP quantification.

An ATP quantification kit employing firefly luciferase (Invitrogen) was used following manufacturer's guidelines with a slight modification to the working solution. To increase assay sensitivity, 3.5 μL of luciferase was added to the ATP working solution as opposed to 2.5 μL. ATP was quantified by adding 270 μL of ATP working solution to a nitric acid washed glass test tube. Thirty μL of sample was added and mixed by gently pipetting up and down and incubated at room temperature for one minute. Following incubation, test tubes were placed in a luminometer (Lu-mini, Vitl Life Solutions, Ashland, VA) and measurements were recorded. Background assays were performed in triplicate using blank medium treated the same as samples and values were subtracted from experimental samples. A standard curve to relate ATP concentration to luminescence was generated using an ATP stock (Invitrogen) and the same volumes and ATP working solution described above.

### RNA extraction and cDNA synthesis

Mid-log phase cultures of *Hydrogenobacter* RSW1 were harvested by filtration using an autoclaved glass filter tower. Cells were filtered onto 47 mm diameter, 0.2 μm pore size filters (Pall, Port Washington, NY). Filters were then placed into sterile 50 mL Falcon tubes and 750 μL of TRIzol extraction reagent (Invitrogen) was then added. The filtered biomass and TRIzol were then flash frozen in liquid nitrogen and stored at − 80 °C until further processing. Detailed instructions for TRIzol extractions can be found in Supplemental Material. RNA was quantified using the Qubit BR RNA quantification kit (Invitrogen) and was quality checked using a NanoDrop spectrophotometer (ThermoFisher Scientific, Waltham, MA). The absence of PCR-amplifiable DNA was confirmed by PCR amplification using universal 16S rRNA primers

(515 F (5′- GTGYCAGCMGCCGCGGTAA-3′) and 806 R (5′- GGACTACNVGGGTWTCTAAT′)) and was visualized through gel electrophoresis. The thirty five cycle PCR was conducted at an annealing temperature of 50 °C with 5 μL of template. After confirming the quality of RNA and the absence of PCR amplifiable DNA, RNA was converted into cDNA using the iScript Select cDNA synthesis kit (Bio-Rad Laboratories, Hercules, CA) according to the manufacturer's protocol.

### qPCR

cDNA was subject to quantitative PCR (qPCR) using four different primer sets designed using the NCBI Primer BLAST tool. Each primer set was designed to amplify a specific gene of interest (GOI), including primers for the *rpoB* subunit, sulfur reductase subunit A (*sreA*), and cyctochrome c oxidase subunit 1 genes (*cox*1, *cox*2). Primer sequences, the genes they target, and primer annealing temperatures are reported in Supplementary Data 1. qPCR was conducted using the SYBR Green Supermix (Bio-Rad Laboratories) in a final volume of 20 μL. One μL of cDNA product and 0.5 μL of both the forward and reverse primers (10 mM stock concentration) were added to each reaction and reactions were subject to the following cycling conditions in the CFX Connect Real-time system (Bio-Rad): Initial denaturing at 95 °C for one minute, followed by 35 cycles of 95 °C for 30 s, annealing at specified temperature (Supplementary Data 1) for one minute, and extension at 72 °C for 30 s, with a plate read step at the end of each cycle. This was followed by a melt curve from 65–95 °C with 0.5 °C increases every 5 s. Details for creating plasmid standards can be found in the Supplemental Materials document. Negative control qPCR reactions were performed in the absence of added cDNA.

### Reporting summary

Further information on research design is available in the Nature Portfolio Reporting Summary linked to this article.

## Data availability

All data generated or analyzed during this study are included in the text and figures of this published article and its Supplementary Materials. Raw values for all figures in the manuscript and supplemental materials can be found in the Source Data file. RSW1 genomic sequencing is available through NCBI under Biosample accession number SAMN40709733. Source data are provided with this paper.

## References


1. Reysenbach, A.-L. et al. Aquificales in Yellowstone National Park. (2006).
2. Takacs-vesbach, C. et al. Metagenome sequence analysis of filamentous microbial communities obtained from geochemically distinct geothermal channels reveals specialization of three Aquificales lineages. *Fron. Microbiol.* **4**, 84 (2013).
3. Hou, W. et al. A comprehensive census of microbial diversity in hot springs of Tengchong, Yunnan Province China using 16S rRNA gene pyrosequencing. *PLoS One* **8**, e53350 (2013).
4. Song, Z.-Q. et al. Bacterial and archaeal diversities in Yunnan and Tibetan hot springs, China. *Environ. Microbiol.* **15**, 1160–1175 (2013).
5. Colman, D. R. et al. Tectonic and geological setting influence hot spring microbiology. *Environ. Microbiol.* **25**, 2481–2497 (2023).
6. Brock, T. D. *Thermophilic Microorganisms and Life at High Temperatures*. (Springer-Verlag, 1978).
7. Castenholz, R. W. The thermophilic Cyanophytes of Iceland and the upper temperature limit *J. Phycol* **5**, 360–368 (1969).
8. Huber, R. & Eder, W. in *The Prokaryotes*: *Volume* 7: *Proteobacteria: Delta, Epsilon Subclass* (eds Martin Dworkin et al.) 925-938 (Springer New York, 2006).
9. L'Haridon, S. et al. *Desulfurobacterium thermolithotrophum* gen. nov., sp. nov., a novel autotrophic, sulphur-reducing bacterium isolated from a deep-sea hydrothermal vent. *IJSEM* **48**, 701–711 (1998).
10. Nakagawa, S. et al. *Sulfurihydrogenibium yellowstonense* sp. nov., an extremely thermophilic, facultatively heterotrophic, sulfur-oxidizing bacterium from Yellowstone National Park, and emended descriptions of the genus *Sulfurihydrogenibium, Sulfurihydrogenibium subterraneum* and *Sulfurihydrogenibium azorense*. *IJSEM* **55**, 2263–2268 (2005).
11. Takai, K., Kobayashi, H., Nealson, K. H. & Horikoshi, K. *Sulfurihydrogenibium subterraneum* gen. nov., sp. nov., from a subsurface hot aquifer. *IJSEM* **53**, 823–827 (2003).
12. Kawasumi, T., Igarashi, Y., Kodama, T. & Minoda, Y. *Hydrogenobacter thermophilus* gen. nov. sp., an extremely thermophilic, aerobic, hydrogen-oxidizing bacterium. *IJSEM* **34**, 5–10 (1984).
13. Takai, K., Komatsu, T. & Horikoshi, K. *Hydrogenobacter subterraneus* sp. nov., an extremely thermophilic, heterotrophic bacterium unable to grow on hydrogen gas, from deep subsurface geothermal water. *IJSEM* **51**, 1425–1435 (2001).
14. Aguiar, P., Beveridge, T. J. & Reysenbach, A.-L. Sulfurihydrogenibium azorense, sp. nov., a thermophilic hydrogen-oxidizing microaerophile from terrestrial hot springs in the Azores. *IJSEM* **54**, 33–39 (2004).
15. Suzuki, M., Cui, Z. J., Ishii, M. & Igarashi, Y. Nitrate respiratory metabolism in an obligately autotrophic hydrogen-oxidizing bacterium, *Hydrogenobacter thermophilus* TK-6. *Arch. Microbiol.* **175**, 75–78 (2001).
16. Kawasumi, T., Igarashi, Y., Kodama, T. & Minoda, Y. Isolation of strictly thermophilic and obligately autotrophic hydrogen bacteria. *Agric. Biol. Chem.* **44**, 1985–1986 (1980).
17. McCleskey, R. B., Ball, J. W., Nordstrom, D. K., Holloway, J. M. & Taylor, H. E. Water-chemistry data for selected springs, geysers, and streams in Yellowstone National Park Wyoming, 2001-2002. Report No. 2004-1316, (2005).
18. Nye, J. J., Shock, E. L. & Hartnett, H. E. A novel PARAFAC model for continental hot springs reveals unique dissolved organic carbon compositions. *Org. Geochem.* **141**, 103964 (2020).
19. Fournier, R. O. Geochemistry and dynamics of the Yellowstone National Park hydrothermal system. *Annu. Rev. Earth Planet. Sci.* **17**, 13–53 (1989).
20. Nordstrom, K. D., McCleskey, B. R. & Ball, J. W. Sulfur geochemistry of hydrothermal waters in Yellowstone National Park: IV Acid–sulfate waters. *Appl. Geochem.* **24**, 191–207 (2009).
21. Nordstrom, D. K., McCleskey, B. R. & Ball, J. W. Ground water to surface water: chemistry of thermal outflows in Yellowstone National Park. In *Geothermal Biology and Geochmistry in Yellowstone National Park* (eds Inskeep, W. P. & McDermott, T. R.) 73–94 (Montana State University, Bozeman, Montana, USA, 2005).
22. Donahoe-Christiansen, J., D'Imperio, S., Jackson, C. R., Inskeep, W. P. & McDermott, T. R. Arsenite-oxidizing *Hydrogenobaculum* strain isolated from an acid-sulfate-chloride geothermal spring in Yellowstone National Park. *Appl. Environ. Microbiol.* **70**, 1865–1868 (2004).
23. Romano, C. et al. Comparative genomic analysis of phylogenetically closely related *Hydrogenobaculum* sp. ssolates from Yellowstone National Park. *Appl. Environ. Microbiol.* **79**, 2932–2943 (2013).
24. Stohr, R., Waberski, A., Völker, H., Tindall, B. J. & Thomm, M. *Hydrogenothermus marinus* gen. nov., sp. nov., a novel thermophilic hydrogen-oxidizing bacterium, recognition of *Calderobacterium hydrogenophilum* as a member of the genus Hydrogenobacter and proposal of the reclassification of *Hydrogenobacter acidophilus* as *Hydrogenobaculum acidophilum* gen. nov., comb. nov., in the phylum 'Hydrogenobacter/Aquifex'. *IJSEM* **51**, 1853–1862 (2001).
25. D'Imperio, S. et al. Relative Importance of H2 and H2S as Energy Sources for Primary Production in Geothermal Springs. *Appl. Environ. Microbiol.* **74**, 5802–5808 (2008).

26. Caldwell, S. L., Liu, Y., Ferrera, I., Beveridge, T. & Reysenbach, A.-L. Thermocrinis minervae sp. nov., a hydrogen- and sulfur-oxidizing, thermophilic member of the Aquificales from a Costa Rican terrestrial hot spring. *IJSEM* **60**, 338–343 (2010).
27. Dodsworth, J. A., Ong, J. C., Williams, A. J., Dohnalkova, A. C. & Hedlund, B. P. *Thermocrinis jamiesonii* sp. nov., a thiosulfate-oxidizing, autotropic thermophile isolated from a geothermal spring. *IJSEM* **65**, 4769–4775 (2015).
28. Huber, R. et al. *Thermocrinis ruber* gen. nov., sp. nov., a pink-filament-forming hyperthermophilic bacterium isolated from Yellowstone National Park. *Appl. Environ. Microbiol.* **64**, 3576–3583 (1998).
29. Havig, J. R., Raymond, J., Meyer-Dombard, D. A. R., Zolotova, N. & Shock, E. L. Merging isotopes and community genomics in a siliceous sinter-depositing hot spring. *J. Geophys. Res: Biogeosci*. **116**. https://doi.org/10.1029/2010JG001415 (2011).
30. Meyer-Dombard, D. R. et al. Hydrothermal ecotones and streamer biofilm communities in the Lower Geyser Basin, Yellowstone National Park. *Environ. Microbiol.* **13**, 2216–2231 (2011).
31. Gardner, W. P., Susong, D. D., Solomon, D. K. & Heasler, H. P. Using environmental tracers and numerical simulation to investigate regional hydrothermal basins—Norris Geyser Basin area, Yellowstone National Park, USA. *J. Geophys. Res: Solid Earth* **118**, 2777–2787 (2013).
32. Sims, K. W. W. et al. The dynamic influence of subsurface geological processes on the assembly and diversification of thermophilic microbial communities in continental hydrothermal systems. *Geochimica et. Cosmochimica Acta* **362**, 77–103 (2023).
33. Colman, D. R. et al. Ecological differentiation in planktonic and sediment-associated chemotrophic microbial populations in Yellowstone hot springs. *FEMS Microbiol. Ecol*. **92** https://doi.org/10.1093/femsec/fiw137 (2016).
34. Fernandes-Martins, M. C. et al. Ecological dichotomies arise in microbial communities due to mixing of deep hydrothermal waters and atmospheric gas in a circumneutral hot spring. *Appl. Environ. Microbiol.* **87**, e01598–01521 (2021).
35. Power, J. F. et al. Microbial biogeography of 925 geothermal springs in New Zealand. *Nat. Commun.* **9**, 2876 (2018).
36. Cole, J. K. et al. Sediment microbial communities in Great Boiling Spring are controlled by temperature and distinct from water communities. *ISME J.* **7**, 718–729 (2013).
37. Power, J. F. et al. A genus in the bacterial phylum Aquificota appears to be endemic to Aotearoa-New Zealand. *Nat. Commun.* **15**, 179 (2024).
38. Keller, L. M., Colman, D. R. & Boyd, E. S. An active microbiome in Old Faithful geyser. *PNAS Nexus* **2** https://doi.org/10.1093/pnasnexus/pgad066 (2023).
39. Deckert, G. et al. The complete genome of the hyperthermophilic bacterium Aquifex aeolicus. *Nature* **392**, 353–358 (1998).
40. Guiral, M. et al. A membrane-bound multienzyme, hydrogen-oxidizing, and sulfur-reducing complex from the hyperthermophilic bacterium *Aquifex aeolicus*. *J. Biol. Chem.* **280**, 42004–42015 (2005).
41. Ball, J. W. et al. Water-chemistry data for selected springs, geysers, and streams in Yellowstone National Park, Wyoming, 1999-2000. Report No. 2002-382, (Reston, VA, 2002).
42. Wilson, C. L., Hinman, N. W., Cooper, W. J. & Brown, C. F. Hydrogen peroxide cycling in surface geothermal waters of Yellowstone National Park. *Environ. Sci. Technol.* **34**, 2655–2662 (2000).
43. Fernandes-Martins, M. C., Colman, D. R. & Boyd, E. S. Relationships between fluid mixing, biodiversity, and chemosynthetic primary productivity in Yellowstone hot springs. *Environ. Microbiol.* **25**, 1022–1040 (2023).
44. Lindsay, M. R. et al. Subsurface processes influence oxidant availability and chemoautotrophic hydrogen metabolism in Yellowstone hot springs. *Geobiology* **16**, 674–692 (2018).
45. Woodcroft, B. J. et al. SingleM and Sandpiper: Robust microbial taxonomic profiles from metagenomic data. *bioRxiv*, 2024.2001.2030.578060 https://doi.org/10.1101/2024.01.30.578060 (2024).
46. Kryukov, V. R., Savel'eva, N. D. & Pusheva, M. A. *Calderobacterium hydrogenophilum* new genus new species an extreme thermophilic hydrogen bacterium and its hydrogenase activity. *Mikrobiologiya* **52**, 781–788 (1983).
47. Oshima, K., Chiba, Y., Igarashi, Y., Arai, H. & Ishii, M. Phylogenetic position of aquificales based on the whole genome sequences of six aquificales species. *Int J. Evol. Biol.* **2012**, 859264 (2012).
48. Cao, J. et al. Desulfurobacterium indicum sp. nov., a thermophilic sulfur-reducing bacterium from the Indian Ocean. *IJSEM* **67**, 1665–1668 (2017).
49. Pérez-Rodríguez, I. et al. *Phorcysia thermohydrogeniphila* gen. nov., sp. nov., a thermophilic, chemolithoautotrophic, nitrate-ammonifying bacterium from a deep-sea hydrothermal vent. *IJSEM* **62**, 2388–2394 (2012).
50. Huber, H., Diller, S., Horn, C. & Rachel, R. *Thermovibrio ruber* gen. nov., sp. nov., an extremely thermophilic, chemolithoautotrophic, nitrate-reducing bacterium that forms a deep branch within the phylum Aquificae. *IJSEM* **52**, 1859–1865 (2002).
51. Jelen, B., Giovannelli, D., Falkowski, P. G. & Vetriani, C. Elemental sulfur reduction in the deep-sea vent thermophile, Thermovibrio ammonificans. *Environ. Microbiol.* **20**, 2301–2316 (2018).
52. Takai, K., Nakagawa, S., Sako, Y. & Horikoshi, K. *Balnearium lithotrophicum* gen. nov., sp. nov., a novel thermophilic, strictly anaerobic, hydrogen-oxidizing chemolithoautotroph isolated from a black smoker chimney in the Suiyo Seamount hydrothermal system. *IJSEM* **53**, 1947–1954 (2003).
53. Eder, W. & Huber, R. New isolates and physiological properties of the Aquificales and description of *Thermocrinis albus* sp. nov. *Extremophiles* **6**, 309–318 (2002).
54. Hedlund, B. P. et al. Isolation of diverse members of the Aquificales from geothermal springs in Tengchong, China. *Front. Microbiol*. **6** https://doi.org/10.3389/fmicb.2015.00157 (2015).
55. Hügler, M., Huber, H., Molyneaux, S. J., Vetriani, C. & Sievert, S. M. Autotrophic CO2 fixation via the reductive tricarboxylic acid cycle in different lineages within the phylum Aquificae: evidence for two ways of citrate cleavage. *Environ. Microbiol.* **9**, 81–92 (2007).
56. Reysenbach, A.-L. et al. Complete and draft genome sequences of six members of the Aquificales. *J. Bacteriol.* **191**, 1992–1993 (2009).
57. Friedrich, C. G., Bardischewsky, F., Rother, D., Quentmeier, A. & Fischer, J. Prokaryotic sulfur oxidation. *Curr. Opini. Microbiol.* **8**, 253–259 (2005).
58. Amenabar, M. J., Colman, D. R., Poudel, S., Roden, E. E. & Boyd, E. S. Electron acceptor availability alters carbon and energy metabolism in a thermoacidophile. *Environ. Microbiol.* **20**, 2523–2537 (2018).
59. Laska, S., Lottspeich, F. & Kletzin, A. Membrane-bound hydrogenase and sulfur reductase of the hyperthermophilic and acidophilic archaeon *Acidianus ambivalens*. *Microbiol* **149**, 2357–2371 (2003).
60. Søndergaard, D., Pedersen, C. N. S. & Greening, C. HydDB: A web tool for hydrogenase classification and analysis. *Sci. Rep.* **6**, 34212 (2016).
61. Siebers, B. et al. Reconstruction of the central carbohydrate metabolism of *Thermoproteus tenax* by use of genomic and biochemical data. *J. Bacteriol.* **186**, 2179–2194 (2004).
62. Siebers, B. et al. The complete genome sequence of *Thermoproteus tenax*: A physiologically versatile member of the Crenarchaeota. *PLOS ONE* **6**, e24222 (2011).
63. Dirmeier, R., Keller, M., Frey, G., Huber, H. & Stetter, K. O. Purification and properties of an extremely thermostable membrane-bound sulfur-reducing complex from the hyperthermophilic *Pyrodictium abyssi*. *Eur. J. Biochem.* **252**, 486–491 (1998).

64. Luther, G. W. et al. Thermodynamics and kinetics of sulfide oxidation by oxygen: a look at inorganically controlled reactions and biologically mediated processes in the environment. *Front. Microbiol.* **2** https://doi.org/10.3389/fmicb.2011.00062 (2011).
65. Millero, F. J., Hubinger, S., Fernandez, M. & Garnett, S. Oxidation of H2S in seawater as a function of temperature, pH, and ionic strength. *Environ. Sci. Technol.* **21**, 439–443 (1987).
66. Bonch-Osmolovskaya, E. A. Bacterial sulfur reduction in hot vents. *FEMS Microbiol. Rev.* **15**, 65–77 (1994).
67. Amend, J. P. & Shock, E. L. Energetics of overall metabolic reactions of thermophilic and hyperthermophilic Archaea and Bacteria. *FEMS Microbiol. Rev.* **25**, 175–243 (2001).
68. Han, P. & Bartels, D. M. Temperature dependence of oxygen diffusion in H2O and D2O. *J. Phys. Chem.* **100**, 5597–5602 (1996).
69. Hirai, T., Osamura, T., Ishii, M. & Arai, H. Expression of multiple $cbb_3$ cytochrome c oxidase isoforms by combinations of multiple isosubunits in *Pseudomonas aeruginosa*. *Proc. Natl. Acad. Sci.* **113**, 12815–12819 (2016).
70. Canfield, D. E. et al. A Cryptic Sulfur Cycle in Oxygen-Minimum–Zone Waters off the Chilean Coast. *Science* **330**, 1375–1378 (2010).
71. Mills, J. V., Antler, G. & Turchyn, A. V. Geochemical evidence for cryptic sulfur cycling in salt marsh sediments. *Earth Planet. Sci. Lett.* **453**, 23–32 (2016).
72. McCleskey, R. B., et al. (Geological Survey Online Database, 2014).
73. Burggraf, S., Olsen, G. J., Stetter, K. O. & Woese, C. R. A Phylogenetic Analysis of Aquifex pyrophilus. *Sys. Appl. Microbiol.* **15**, 352–356 (1992).
74. Anbar, A. D. et al. A Whiff of Oxygen Before the Great Oxidation Event? *Science* **317**, 1903–1906 (2007).
75. Canfield, D. E. & Des Marais, D. J. Aerobic Sulfate Reduction in Microbial Mats. *Science* **251**, 1471–1473 (1991).
76. Hastings, D. & Emerson, S. Sulfate reduction in the presence of low oxygen levels in the water column of the Cariaco Trench1,2. *Limnol. Oceanogr.* **33**, 391–396 (1988).
77. Marschall, C., Frenzel, P. & Cypionka, H. Influence of oxygen on sulfate reduction and growth of sulfate-reducing bacteria. *Arch. Microbiol.* **159**, 168–173 (1993).
78. Widdel, F., Kohring, G.-W. & Mayer, F. Studies on dissimilatory sulfate-reducing bacteria that decompose fatty acids. *Arch. Microbiol.* **134**, 286–294 (1983).
79. Atlas, R. M. *Handbook of Microbiological Media: Second Edition*. (CRC-Press, 1996).
80. Morono, Y., Terada, T., Kallmeyer, J. & Inagaki, F. An improved cell separation technique for marine subsurface sediments: applications for high-throughput analysis using flow cytometry and cell sorting. *Environ. Microbiol.* **15**, 2841–2849 (2013).
81. Nurk, S., Meleshko, D., Korobeynikov, A. & Pevzner, P. A. metaSPAdes: a new versatile metagenomic assembler. *Genome Res.* **27**, 824–834 (2017).
82. Seemann, T. Prokka: rapid prokaryotic genome annotation. *Bioinformatics* **30**, 2068–2069 (2014).
83. Kanehisa, M. & Goto, S. KEGG: Kyoto Encyclopedia of Genes and Genomes. *Nucleic Acids Res.* **28**, 27–30 (2000).
84. Moriya, Y., Itoh, M., Okuda, S., Yoshizawa, A. C. & Kanehisa, M. KAAS: an automatic genome annotation and pathway reconstruction server. *Nucleic Acids Res.* **35**, W182–W185 (2007).
85. Rodriguez-R, L. & Konstantinidis, K. The enveomics collection: a toolbox for specialized analyses of microbial genomes and metagenomes. https://doi.org/10.7287/peerj.preprints.1900v1 (2016).
86. Colman, D. R. et al. Covariation of hot spring geochemistry with microbial genomic diversity, function, and evolution. *Nat. Commun.* **15**, 7506 (2024).
87. Sievers, F. et al. Fast, scalable generation of high-quality protein multiple sequence alignments using Clustal Omega. *Mol. Syst. Biol.* **7**, 539 (2011).
88. Nguyen, L.-T., Schmidt, H. A., von Haeseler, A. & Minh, B. Q. IQ-TREE: a fast and effective stochastic algorithm for estimating maximum-likelihood phylogenies. *Mol. Biol. Evol.* **32**, 268–274 (2014).
89. Letunic, I. & Bork, P. Interactive Tree Of Life (iTOL) v5: an online tool for phylogenetic tree display and annotation. *Nucleic Acids Res.* **49**, 293–296 (2021).
90. Moest, R. R. Hydrogen sulfide determination by the methylene blue method. *Anal. Chem.* **47**, 1204–1205 (1975).
91. Kolmert, Å., Wikström, P. & Hallberg, K. B. A fast and simple turbidimetric method for the determination of sulfate in sulfate-reducing bacterial cultures. *J. Microbiol. Methods* **41**, 179–184 (2000).

## Acknowledgements

This work was supported by a grant from the National Aeronautics and Space Administration (NASA) to D.R.C. and E.S.B. (80NSSC19M0150) and by a grant from the W.M. Keck Foundation to E.S.B (MSU-2019). The authors are grateful to Drs. Maximiliano Amenabar and Melody Lindsay for assistance in sample and data collection in 2017. The authors also thank the National Park Service for permitting and sample collection under permit number YELL-SCI-5544.

## Author contributions

The study was designed by L.M.K and E.S.B.; All experiments were performed by L.M.K; Data analysis was done by L.M.K and E.S.B.; L.M.K, D.R.C., and E.S.B. contributed to writing the manuscript.

## Competing interests

The authors declare no competing interests.

## Additional information

**Supplementary information** The online version contains supplementary material available at https://doi.org/10.1038/s41467-025-56418-4.

**Correspondence** and requests for materials should be addressed to Eric S. Boyd.

**Peer review information** *Nature Communications* thanks the anonymous reviewer(s) for their contribution to the peer review of this work. A peer review file is available.

**Reprints and permissions information** is available at http://www.nature.com/reprints

**Publisher's note** Springer Nature remains neutral with regard to jurisdictional claims in published maps and institutional affiliations.

**Open Access** This article is licensed under a Creative Commons Attribution-NonCommercial-NoDerivatives 4.0 International License, which permits any non-commercial use, sharing, distribution and reproduction in any medium or format, as long as you give appropriate credit to the original author(s) and the source, provide a link to the Creative Commons licence, and indicate if you modified the licensed material. You do not have permission under this licence to share adapted material derived from this article or parts of it. The images or other third party material in this article are included in the article's Creative Commons licence, unless indicated otherwise in a credit line to the material. If material is not included in the article's Creative Commons licence and your intended use is not permitted by statutory regulation or exceeds the permitted use, you will need to obtain permission directly from the copyright holder. To view a copy of this licence, visit http://creativecommons.org/licenses/by-nc-nd/4.0/.

© The Author(s) 2025